Digital Front End Algorithms for Sub-Band Full Duplex

SYEDA MIDHAT HASAN RIZVI AND KHALED AL KHATEEB
MASTER´S THESIS
DEPARTMENT OF ELECTRICAL AND INFORMATION TECHNOLOGY
FACULTY OF ENGINEERING | LTH | LUND UNIVERSITY

Digital Front End Algorithms for Sub-Band Full Duplex

Master's Thesis

By

Syeda Midhat Hasan Rizvi and Khaled Al Khateeb

Department of Electrical and Information Technology
Faculty of Engineering, LTH, Lund University
SE-221 00 Lund, Sweden

LUND UNIVERSITY

ERICSSON

2022

Abstract

Sub-band full duplex is a new communication scheme technology, where a single frequency band is partitioned into sub-bands for down-link (DL) and up-link(UL) transmissions, and both can take place simultaneously. The idea behind the sub-band full duplex development is to improve the throughput, coverage and reduce the latency of the UL communication by allowing the UL reception during the DL transmission. Several integrated ways enable sub-bands frequency isolation, such as antenna's spatial isolation and signal processing techniques to mitigate interferences.

The main challenge for a gNodeB, capable of a full duplex, is self-interference mitigation. A self-interference mitigation technique enables a radio transceiver to transmit and receive simultaneously on a single channel.

During the design process, Digital Front End (DFE) of the Radio Near algorithm (RNA) is considered the main part of the study (with certain limitations) as it involves the algorithms with the use of MATLAB, which are used to mitigate the distortion caused by radio hardware imperfections. Signal processing algorithms are performed on the transmitter side and receiver side of DFE. The transmitter side includes the Crest Factor Reduction (CFR) block followed by Digital Pre-Distortion (DPD) block before the Power amplifier (PA) to linearize PA output. The transmit path also includes the feedback path for DPD which is used for the linearization of PA. The algorithms for CFR block namely Turbo Clipping and Peak Cancelation Crest Factor Reduction (PC-CFR) were developed and compared for the performance in terms of Adjacent Channel Leakage Ratio (ACLR) and Error Vector Magnitude (EVM). The algorithm for DPD namely 2-stage frequency selective DPD is implemented along with the legacy DPD technique, and the performance was evaluated in terms of ACLR and EVM.

Finally, the Self-interference cancelation (SIC) algorithm is implemented at the receiver chain side. Signal to Interference Noise Ratio (SINR) is measured for different Signal to Noise Ratios (SNRs) and different RF cancellations levels to evaluate the system performance at gNodeB.

Acknowledgments

We would like to express our gratitude and thanks to Ericsson and Lund University who honored us to participate in this cutting-edge thesis work. The collaboration between Ericsson and LTH is a blessing for all the students.

First, a great thank goes to all people at Ericsson AB, Lund. To our main supervisor at Ericsson, Mohamed Hamid, for his boundless guidance and support. To Magnus Nilsson B and Martin Isberg for the unlimited help, they offered during the project.

Special thanks go to our supervisors Aleksei Fedorov and Juan Sanchez and examiner Michael Lentmaier at Lund University for their great help and support.

Finally, to our lovely families and friends, thank you for support and encouragement.

Syeda Midhat Hasan Rizvi Khaled Al Khateeb

Contents

List of Acronyms and Abbreviations

ACLR	Adjacent Channel Leakage Ratio
ADC	Analog to Digital Converter
AM/AM	Amplitude to Amplitude
AM/PM	Amplitude to Phase
AWGN	Additive White Gaussian Noise
BER	Bit Error Rate
CAF	Clipping and Filtering
CFR	Crest Factor Reduction
CLI	Cross Line Interference
DFE	Digital front end
DL	Downlink
DPD	Digital Pre-Distortion
DLA	Direct Learning Architecture
EVM	Error Vector Magnitude
FDD	Frequency Division Duplex
FIR	Finite Impulse Response
FR1	Frequency Range 1
FR2	Frequency Range 2
GSM	Global System for Mobile communications
ILA	Indirect Learning Architecture
ILC	Iterative Learning Control
LTE	Long-Term Evolution

LNA	Low Noise Amplifier
MIMO	Multiple Input Multiple Output
NR	New Radio
NPR	Noise Power Ratio
OFDM	Orthogonal Frequency Division Multiplexing
PA	Power Amplifier
PAPR	Peak to Average Power Ratio
PC	Peak Cancellation
PC-CFR	Peak Cancellation Crest Factor Reduction
PCU	Peak Cancelling Unit
PM	Peak Manager
PSW	Peak Search Window
QAM	Quadrature Amplitude Modulation
RF	Radio Frequency
SBFD	Sub Band Full Duplex
SFFD	Single Frequency Full Duplex
SIC	Self-Interference Cancellation
SINR	Signal to Interference Noise Ratio
SNR	Signal to Noise Ratio
TC	Turbo Clipping
TDD	Time Division Duplex
UEs	Users Equipment's
URLLC	Ultra Reliable Low Latency Communications

UL	Uplink
3GPP	3rd Generation Partnership Project

Popular Science Summary

Wireless communication is a way to transfer information from a sender to a receiver, without any wire or fiber, in the form of electromagnetic waves. The information can be sound, text data, images, etc. The radio spectrum is part of the electromagnetic spectrum with frequencies from 1 Hz to 3,000 GHz and is used in modern telecommunication. Cellular communication is one of these wireless radio technologies that has changed modern society. Users are no longer limited to text messages or voice calls. The use of social media, live video streaming, online gaming, shopping, etc are now in trend which results in the consumption of more and more data. According to the Ericsson Mobility Report Nov. 2022, the average data consumption per smartphone is expected to exceed 19 GB per month in 2023, while only new generation mobile subscriptions will hit 5 billion alone in 2028. To fulfil this demand, new technologies are required, along with the improvement of existing ones.

The evolution of wireless communication is based on providing a better-quality experience and more reliable transmission with the fastest possible speed. With every 10 years passing there is a new generation of communications known as generation G-terminology. This journey of evolution started in 1981 as 1G, and now since 2020, we are in the era of 5G. The next generation is now in the research phase and is expected to be launched in the 2030s. Growing from 5G to 6G with the aim of learning from live 5G networks will play a key role in the standardization and development of 6G.

Modern communication systems send and receive simultaneously to exchange information, this concept of two-way transmission is called full duplex. Frequency division duplex (FDD) and time division duplex (TDD) are two fundamental concepts for full-duplex communication. In FDD, separate frequency bands are used for uplink (phone to the network) and downlink (network to the phone) while in TDD, the same frequency band is used for uplink and downlink but only one link can communicate at a time. Both technologies are used in present communication systems. In FDD, a portion of the frequency spectrum is used as a guard band to separate the uplink data and downlink, which is not an efficient use of an expensive

spectrum while TDD deployment is very complex, and longer guard periods are required to separate the uplink and downlink which affects the capacity of the network.

Sub-band full duplex is a novel idea that has the potential to outperform other duplexing schemes and is one of the candidate technologies for 6G advancements. The idea of the sub-band full duplex technique is to utilize the spectrum efficiently without adding any guard band. This new technique has flavors of both duplexing schemes in terms of benefits and challenges which integrates the FDD scheme inside the TDD scheme to enable simultaneous downlink and uplink transmissions.

Sub-band full duplex has many challenges to consider coming up with some practical solutions. One of the challenges is self-interference when spectral sharing is being deployed for two radios operating in the same frequency band simultaneously. Another challenge lies with the digital front-end electronic devices, like power amplifiers' non-linear behavior that degrades the overall system's efficiency. A digital pre-distortion (DPD) algorithm can be used to correct the non-linearity effect and achieve high power efficiency. This technique helps linearize the power amplifier, minimizing in-band distortion and out-of-band emissions and eventually reaching a reduced bit error rate. Before this technique, another signal processing technique, known as crest factor reduction (CFR), could be required to reduce the peak-to-average power ratio of the downlink signal such that the distortion into the other sub-bands is eliminated or reduced.

This thesis investigates an optimization strategy of DPD and CFR algorithms to reduce the self-interference and hence contribute to a better signal quality at the receiver end.

1. Introduction

1.1. Background and Motivation

Wireless communication is a method of transmitting information from one point to another, without using cables or any physical medium. With the help of wireless communication, the transmitting and receiving operations can be handled over a range of short distance, like a Wi-Fi network, to a very long distance, like satellite communication.

Among the different types of technologies to address wireless communications, we can find cellular communications. In this type of communication, the network serves the users in a distributed way across multiple access points called base transceiver stations (BTSs), or base stations (BSs). In order to guarantee interoperability among devices from different operators, multiple organizations take care of creating technology regulations upon which any cellular component must function. One of the most influential organizations is the 3rd Generation Partnership Project (3GPP), that provides requirements to manage radio access, core networks and service capabilities. The standardization process of 3GPP delivers requirements for the so-called mobile system generations, which are structured in releases. 3GPP thus allows development of stable systems with maximum compatibility, safety, and interoperability. The latest generation under which requirements have been placed by 3GPP has been the fifth generation (5G), with the radio access being referred to as new radio (NR). Besides, a new 5G core network development, 3GPP is responsible for presenting a complete network [2].

In addition, 3GPP standardizes and regulates methods of communications between gNodBs and Users' Equipments (UEs), such as regulating duplexing schemes. Duplexing scheme denotes the separation of transmission and reception over a wireless communication channel. It has two communications modes, half duplex and full duplex communications. In half duplex communication, the two communicating devices cannot transmit and receive at the same time. In full duplex communication, simultaneous transmission and reception is possible for a certain frequency band. Full duplex communication is twice as fast as half duplex, and usually uses two separate channels for supporting simultaneous transmission and reception within a certain frequency band. A frequency band can be defined as a group of frequencies ranging from a lower frequency to a higher frequency, where different frequency bands of the electromagnetic spectrum are allocated for numerous applications. The electromagnetic spectrum is the set of

frequencies that includes all the different shapes of electromagnetic radiation afford in the universe.

In order to allow transmission in both directions, a device (UE) or gNodeB must have a duplex scheme. To provide highest possible flexibility, 5G NR supports various duplexing schemes such as Frequency Division Duplex (FDD), Time Division Duplex (TDD). FDD uses two separate frequency bands, denoted uplink (UL) and downlink (DL) frequency bands. UL (from UE to gNodeB) and DL (from gNodeB to UE) transmission can take place simultaneously. Isolation between DL and UL transmissions is accomplished by transmission/reception filters, known as duplex filters, and an adequately large duplex separation in the frequency domain. So, it does not seem like the most efficient use of an expensive resource like frequency spectrum. Mobile devices that use FDD-based cellular technologies require a duplexer when simultaneously using the UL and DL signals on the same antenna. Duplexer can increase the cost of the receiver [2].

On other hand, TDD uses a single frequency band for both transmission and reception operations in different time slots. UL and DL communication are separated by guard times to prevent overlapping. This guard time is equal to transmit-receive switching time and any transmission delays over the communication path. There are no spectrum guards between the slots used but the precise timing and synchronization system for transmitter and receiver are needed. In some TDD formats, dynamic bandwidth allocation that means duration of time slot can be changed according to the demand. For internet access, DLs times are usually much longer than UL. Although the TDD seems better choice, but FDD is more widely implemented and will continue to dominate the cellular business [14]. In TDD, UL and DL are divided timewise, and the transmission is done in turns, which means that each band waits for its turn. In addition, the partitioning of DL and UL bands needs switching time and affects the network latency which is very crucial for time-critical applications like wide area 5G, mobile mm-Wave, green networks, boundless XR, and Ultra Reliable Low Latency Communications (URLLC) where the latency requirements are often in sub-millisecond.

1.2. Objectives

In order to improve 5G systems latency, a new duplex scheme is proposed by QUALCOMM, it is called Sub Band Full Duplex (SBFD). SBFD is a duplex mode where the TDD carrier split into sub-bands to enable simultaneous transmission and reception in the same time slots. Thus, achieving better UL coverage.

SBFD enables flexible and dynamic UL/DL resource adaptation, which enables rapid traffic variations specifically in dense deployments with a relatively small number of users per cell. It could be a use case for small cells with overlapping coverage to neighbor cells and therefore less influence due to inter-cell interference. Furthermore, with cross sub-band scheduling, the gNodeB could provide simultaneous guarantee of large UL throughput and low latency to meet the requirements of 5G critical applications [1].

Implementation of SBFD systems introduces a few new challenges. One of them is so-called Cross-Link Interference (CLI), which occurs when one gNodeB is transmitting, while another is receiving in the same frequency band. CLI can be remarkable when a gNodeB in UL is interfered by the DL from another gNodeB. Another challenge is so-called Self-Interference (SI), which occur when the signal leaks from the gNodeB transmitter to its own receiver. The focus of this thesis was on mitigating SI at gNodeB. SI at gNodeB can be mitigated by frequency sub-bands spectrum isolation. There are several configurations should be deployed in SBFD systems to isolate sub-bands and then mitigate self-interference, which will be discussed in the next chapters.

2. Duplex Schemes in NR

In this chapter, we look forward to showing the advantages of using SBFD and how it outperforms TDD and FDD schemes. In most cases, the NR duplex scheme is given by the available spectrum allocation. Allocations are often paired for lower frequency bands, where one set of frequencies is used for DL and another separate set of frequencies is used for UL, implicating FDD. On the other hand, allocations are unpaired in the case of higher frequency bands, where both DL and UL happen in the same set of frequencies, separated by the time of DL and UL, implicating TDD as shown in Fig. 2.1.

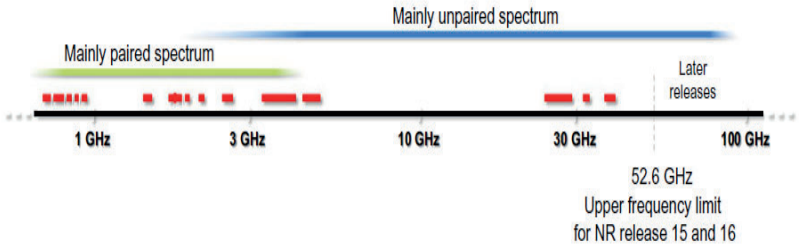

Fig. 2.1 Paired and unpaired spectrum and duplex schemes [2]

NR can operate in both TDD and FDD schemes, where the basic NR is designed such that, it can support both half-duplex and full-duplex operation. In half duplex, the communication device can only transmit or receive at a certain time such as TDD scheme and half-duplex FDD scheme. On the other hand, in full duplex, communication devices can transmit and receive simultaneously such as FDD scheme.

During the development of the NR, one of the main focuses was on providing URLLC services. Besides, increasing bandwidth efficiency and data rates [2]. All these NR design requirements can be enhanced through the SBFD scheme as will be illustrated in the next sections.

2.1. FDD Transmission Scheme

In the case of FDD operation, as shown in Fig. 2.2, there are two different carrier frequencies, one for DL transmission (DL frequency) and one for UL transmission (UL frequency). In each FDD frame, there are ten DL subframes and ten UL subframes, so DL and UL transmission can take place within a cell simultaneously as shown in Fig. 2.2. Isolation between DL and UL transmission can be attained sufficiently by transmission/reception filters, known as duplex filters, and adequately large duplex separation in the frequency domain.

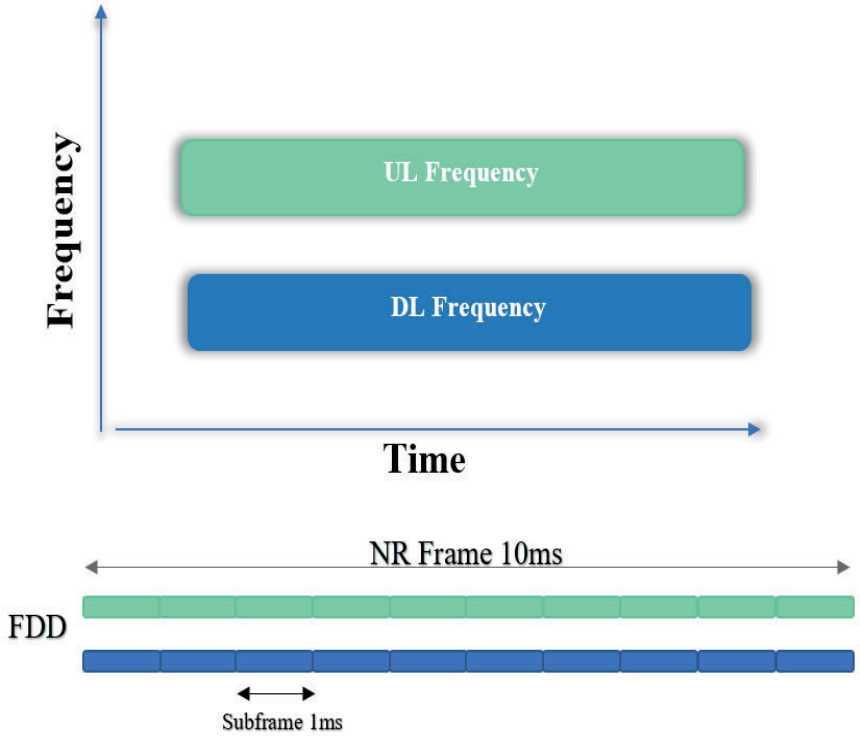

Fig. 2.2 DL and UL transmissions occur in different, efficiently separated frequency bands

Even in case of simultaneous transmission and reception within a cell, in FDD the device can operate in full duplex or half duplex for a certain frequency band, depending on whether it is capable of simultaneous transmission/reception.

The gNodeB can operate in full duplex mode regardless of UE capability. For instance, the gNodeB can transmit to a UE while receiving from another UE simultaneously. Half duplex operation leads to simplified UE implementation due to relaxed duplex filter requirements. This assigns especially for certain frequency bands with a narrow duplex gap. From the network perspective, half duplex operation influences the supported data rates that can be provided from or to a single device as it cannot transmit in all UL transmissions, but the cell capacity is barely influenced as generally it is possible to schedule different terminals in UL and DL transmissions. However, as mentioned above, large duplex separation in FDD leads to inefficient spectrum usage, which can become an issue for future network deployment.

2.2. TDD Transmission Scheme

In the case of TDD operation, as shown in Fig. 2.3, DL and UL transmissions operate on a single carrier frequency, and they are separated in time domain. DL and UL transmissions occur in different, non-overlapping time slots, both from cells and UEs approach. TDD can therefore be categorized as half duplex operation.

TDD is the major duplexing technology for 5G NR, due to the availability of wide spectrum unpaired bands, less complex transceivers design, flexibility in selecting UL to DL data rates ratios, and capability of taking advantage of channel reciprocity. That is, to what level it can be supposed, that the detailed UL channel conditions can be estimated by the device based on DL measurements [2].

In addition, 5G uses dynamic TDD for isolating between DL and UL, where parts of slots can be allocated to either DL or UL dynamically as part of scheduling decision for each time slot, which causes an improvement of the end-user performance compared to the static split between UL and DL resources, where the time domain resources are allocated statically as DL or UL [2].

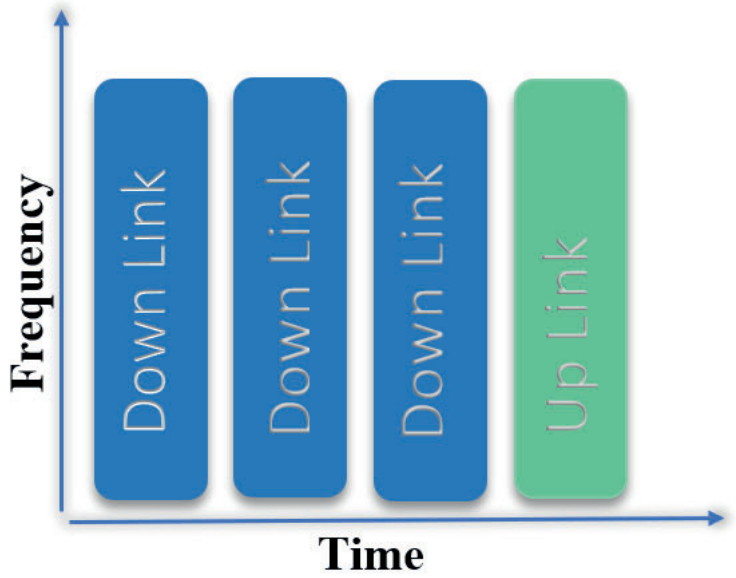

Fig. 2.3 TDD duplex scheme

For example, a high-power DL transmission from a certain cell could notably affect the capability of receiving a weak UL signal from a neighboring cell, and it could also be an interference from UL transmissions affecting the possibility to receive a DL transmission in a neighboring cell as shown in Fig. 2.4, where to the left in Fig. 2.4, DL-to UL interference is explained, which indicates to a situation where the DL transmission in one cell affects the UL reception in another cell, and to the right in Fig. 2.4, UL-to-DL interference is explained, which indicates to UL transmission from one device interfering with DL reception in a neighboring device.

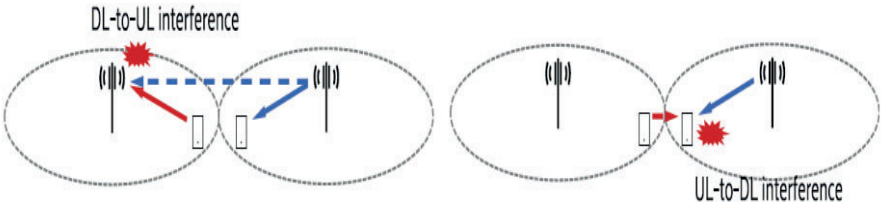

Fig. 2. 4 UL to DL or DL to UL interference in TDD [2]

To switch between DL and UL transmission and vice versa, a guard period is provided, where neither DL nor UL transmission occur. The guard period is obtained by terminating the DL early corresponding to the start of the UL. The required length of the guard period should be large enough to provide the needed time for the circuitry in gNodeBs and the UEs to switch from DL to UL. Furthermore, the length of guard period should be sufficient to prevent any interference at the gNodeB between DL and UL. This is handled by timing advance mechanism, which is a mechanism that controls the UL timing of each device, such that, before the UL-to-DL switch at the gNodeB, the last UL ends before the start of the first DL slot, as shown in Fig. 2.5, where the guard period (timing-advance) must be large enough to let the UE to receive the DL transmission, and then switching to the UL transmission.

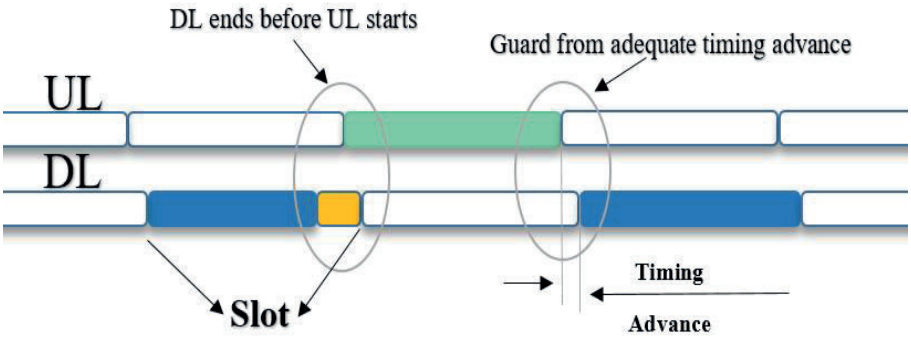

Fig. 2.5 Guard period creation for TDD operation

The environment propagation plays a significant role in deciding the length of guard periods. Besides, the selection of the guard period should consider the interference between gNodeBs, where gNodeBs interference from the DL transmissions in neighboring cells must fade away to a sufficiently low level before the gNodeB can initiate to receive the UL transmissions. Hence, a large guard period may be required as the back end of the DL transmissions from far gNodeBs otherwise may interfere with UL reception [2]. On the other hand, it can be observed that abstracting time periods to switch between the DL and the UL transmissions will decrease the

latency in the TDD transmission scheme, which can lead to obtain some extra advantages as will be discussed in the next section.

2.3. SBFD Transmission Scheme

When it comes to 5G, one is generally thinking about three remarkable classes of use cases: enhanced mobile broadband, massive machine-type communication, and ultra-reliable and low-latency communication.

- Enhanced mobile broadband corresponds to a straightforward development of the users' services of today, allowing even larger data throughput and more enhanced user experience such as providing even higher users' data rates.
- Massive machine-type communication corresponds to services that are represented by a massive number of devices such as remote sensors and monitoring of various equipment. These services consider applications where massive number of inexpensive devices cost and limited devices energy consumption, permitting for very long device battery life of up to at least several years. Usually, each device consumes and generates only a comparatively low amount of data, that is, support for high data rates is less important.
- Ultra-reliable and low-latency communication type-of-services are envisioned to require very low latency and extremely high reliability such as traffic safety, remote control, teleoperation, precision navigation, etc.

To enable 5G NR use cases, a completely new duplex scheme called SBFD has been proposed by Qualcomm to provide lower latency, higher UL throughput, better UL coverage, and enabling better flexibility and dynamism in DL/UL resource adaptation in comparison with the conventional TDD scheme.

SBFD can operate in both Frequency Range 1 (FR1) and Frequency Range 2 (FR2). As can be seen from Fig. 2.6, FR2 includes frequency bands from 24.25 GHz to 52.6 GHz. Communications in this millimeter wave bands have shorter range, but higher available bandwidth than the bands in FR1 which leads to faster data rates in comparison to the data rates that can be provided in FR1 bands. On other hand, FR1 includes frequency bands from 0.45–7.125 GHz, these frequency bands cover much greater distances in comparison to FR2 bands. So, network architectures that work in FR1 bands

require fewer gNodeBs per given area of coverage, which leads to less deployments' costs.

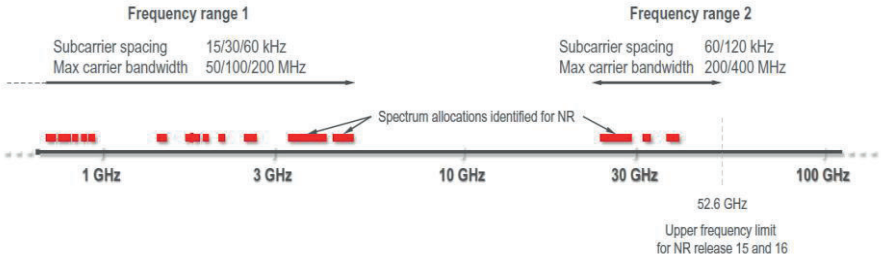

Fig. 2.6 Spectrum identified for NR and subcarrier spacing [2]

In SBFD scheme, the gNodeB can transmit and receive at the same time and on the same spectrum band. As shown in Fig. 2.8, this spectrum band is divided into sub-bands, then these sub-bands are allocated to DL transmission and UL reception. To enable this full duplex communication operation, the gNodeB contains two separated antenna arrays. One array is used for transmitting DL while the second array is used for receiving UL as shown in Fig. 2.7.

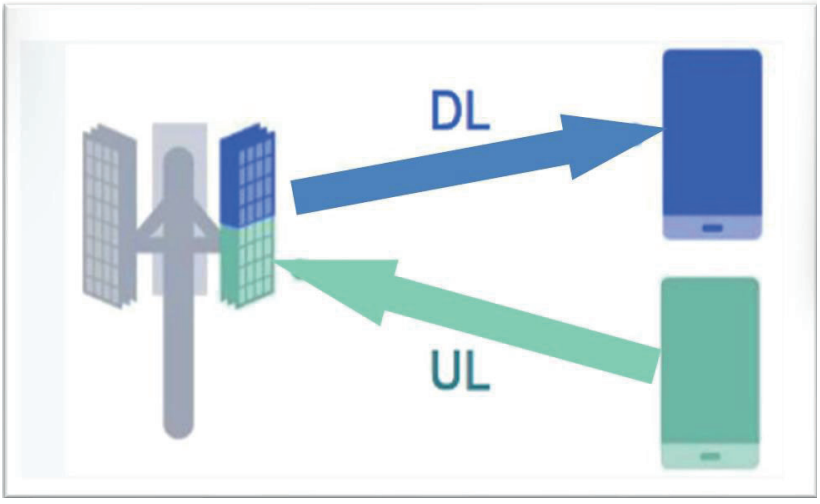

Fig. 2.7 SBFD gNodeB configuration, blue antenna array for transmitting DL and green antenna array for receiving UL simultaneously

As shown in Fig. 2.8, SBFD can be described as a scheme that applies FDD in TDD bands. SBFD enables simultaneous transmission and reception in allocated frequency resources for DL and UL. In SBFD, UL transmissions are increased which will lead to noticeable latency improvement, where UL transmission is included in each time slot instead of waiting three time slots of DL transmissions then receiving one UL transmission as included in TDD scheme (see also Fig. 2. 3). Thus, SBFD presents a latency improvement same as FDD scheme, which is better than TDD due to its limited UL transmissions. Besides, in SBFD with dynamic and flexible DL/UL resource allocation the number of users per cell can be increased or the capacity in general can be increased, where the UL resource allocations are increased.

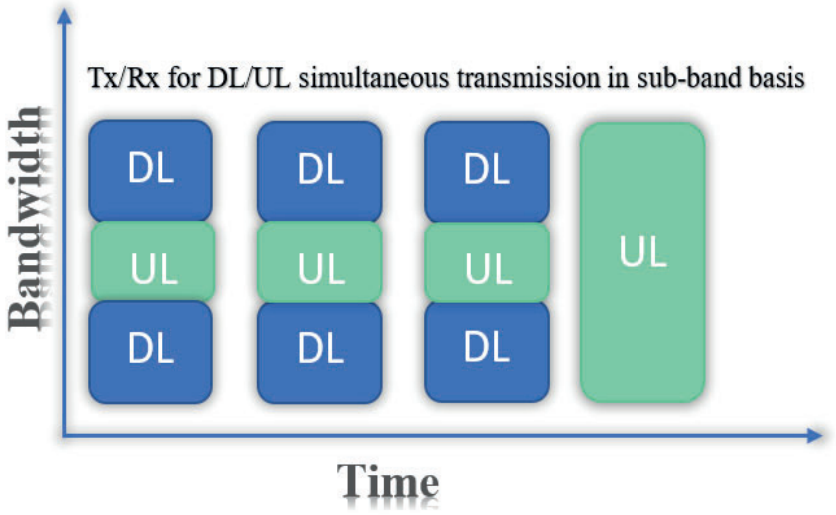

Fig. 2.8 SBFD enables dynamic TDD operation and allows for more flexible service multiplexing as well as improved latency and coverage

In addition, as the UL duty cycles in SBFD are increased, this will lead to extremely good UL coverage same as FDD scheme. Where in TDD the UL coverage is worse than SBFD and FDD due to limited UL transmission slots as shown in Fig. 2.3, where after three allocated DL time slots, we have one allocated UL time slot. While in Fig. 2.8, UL transmissions are included in each time slot in comparison with TDD scheme. Thus, as mentioned before, lower latency could be achieved in SBFD in comparison with TDD.

To provide a better understanding, we illustrate conventional TDD schemes specified in 3GPP documentation in Fig. 2.9 [1]. Fig. 2.9 shows an example of DL and UL transmissions in TDD frame in NR for different communication scenarios. For example, in 5G NR URLLC, UL transmissions are much less than DL transmissions in a time slot, but in SBFD the UL transmissions are increased, which leads also to increase UL throughput and can fulfill URLLC requirements better than conventional 5G transmission structures.

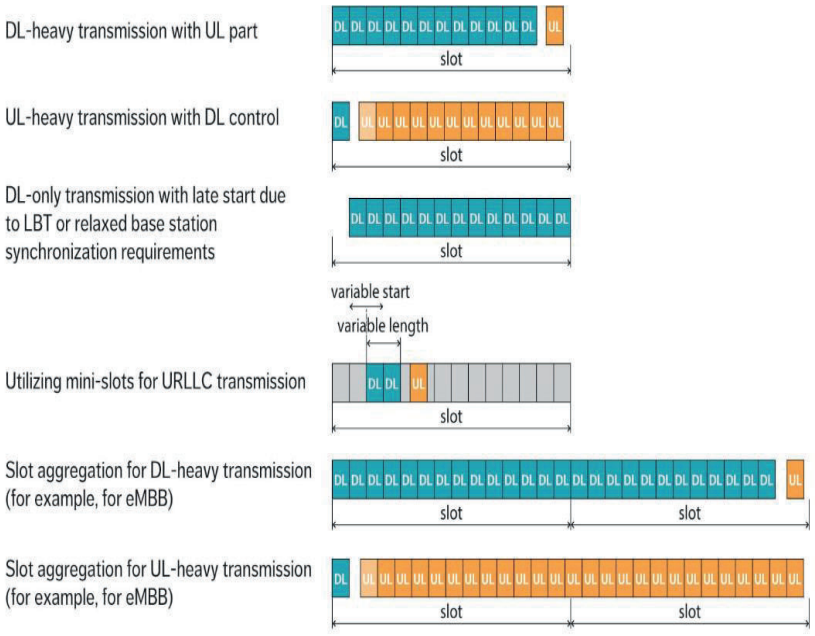

Fig. 2.9 TDD-based frame structure examples for URLLC, operation in unlicensed spectrum [12]

To split between DL and UL resources in the time domain, TDD uses fixed DL/UL time slots across cells. Besides, in TDD either DL or UL can be dynamically allocated in the time domain. This enables tracking fast traffic variations, which are particularly obvious in intensive deployments with a relatively small number of users per gNodeB[2]. While SBFD uses configurable and fixed DL/UL sub-band resources across cells, where splitting between UL and DL can be in both frequency bands and time slots

(see Fig. 2.8), this enables better performance in tracking fast traffic variations. In FDD, as mentioned before, a defined DL and UL carriers are separately allocated, where DL and UL transmission can take place within a cell simultaneously.

In one time slot, SBFD uses only UL band to receive from UEs at the same time of DL transmissions, which allow one hundred usage percent of the available spectrum, no matter of the usage pattern by DL or UL channel. This leads to achieve similar spectrum efficiency as TDD and better than FDD. Besides, as TDD abstracts the need for a frequency guard band between UL and DL channels, SBFD also abstracts the need for frequency guard bands between DL an UL even in between 3rd and 4th time slots, as seen in Fig. 2.8, but in the first three time slots, frequency bands (DL and UL) isolation must be applied to reduce self-interference (SI) and cross line interference (CLI) at gNodeB, that is introduced by Tx sub-band to Rx sub-band leakage, as shown in Fig. 2.10 and Fig. 2.11, where SI occurs when the signal leaks from gNodeB transmitter to its own receiver, or in other words, when DL band interferes with UL band in the same gNodeB. Besides, CLI occurs when one gNodeB or device is transmitting, while another is receiving in the same frequency band. SBFD provides a bias for DL and UL for fixed slots to reduce the intra-cell CLI.

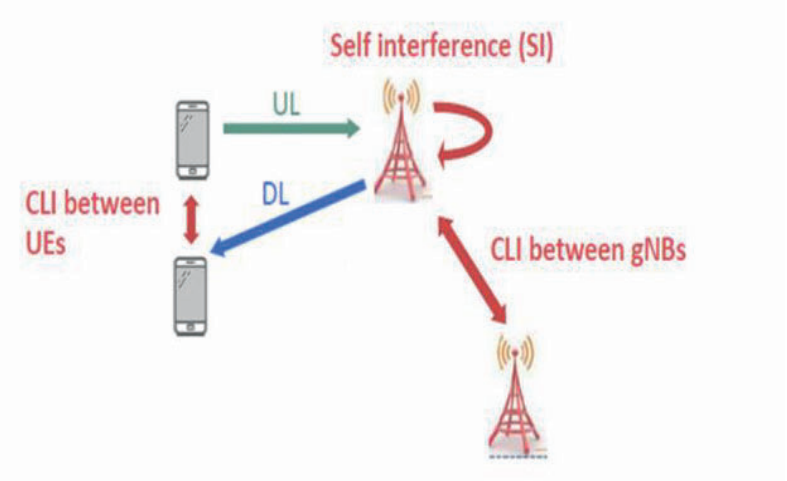

Fig. 2.10 Self-Interference (SI) and Cross Line Interference (CLI) [1]

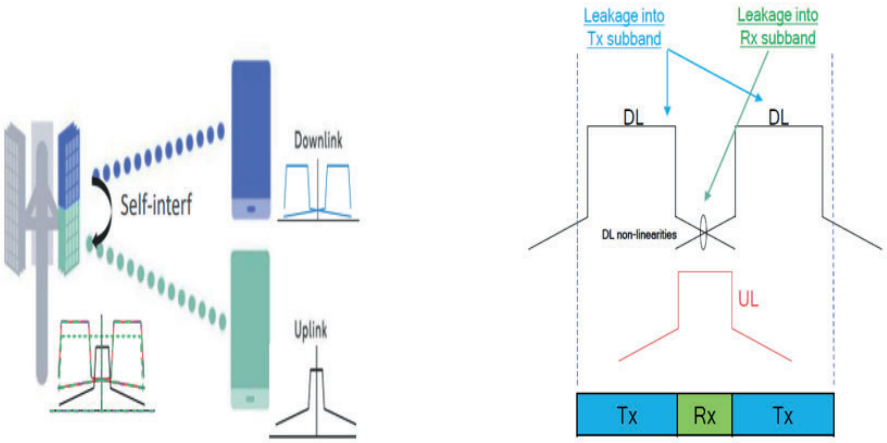

Fig. 2.11 Tx sub-band to Rx sub-band leakage and self-interference [1]

SBFD scheme can be enabled without the presence of Tx to Rx leakage (unwanted coupling from amplified signal in the DL frequency bands inside UL frequency bands) and interferences obstacles by isolating DL and UL frequencies. Multiple configurations are required to isolate UL and DL frequencies in SBFD scheme, as shown in Fig. 2.12, the gNodeB must consist of two antenna arrays panels to enable simultaneous transmission and reception on separated sub-bands at the same time slot, one antenna array for DL transmissions and one for UL receptions, a spatial beam isolation of 80-90 dB is required between Tx and Rx arrays to mitigate self-interference, and then enable an efficient simultaneous transmission and reception at gNodeBs [2].

SBFD uses channel reciprocity same as TDD, where channel reciprocity is an inherit aspect of TDD system which is widely used to get UL/DL channel knowledge from DL/UL channel measurements without additional feedback, or in other words, with channel reciprocity the transmitter and receiver of one wireless link can observe the same channel simultaneously. SBFD provides pre-coding by using channel reciprocity, where pre-coding is a mechanism that exploits transmit diversity by carrying the information stream, which means that the transmitter sends the coded information to the receiver to attain pre-knowledge of the channel. The receiver does not have to know the channel state information. This mechanism will reduce the corrupted influence of the communication channel.

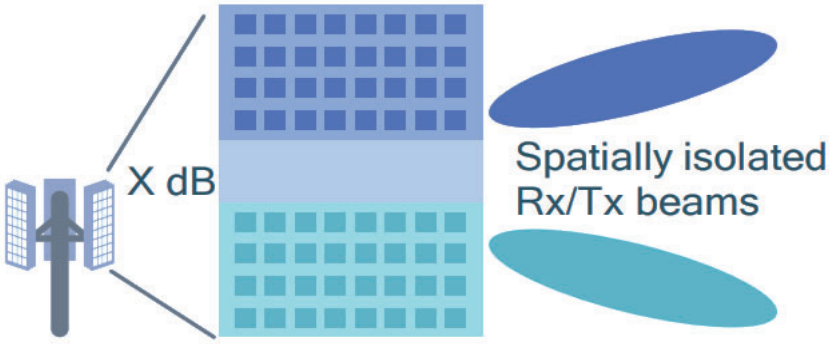

Fig. 2.12 Antenna spatial and beam isolations, the blue antenna array for transmitting (Tx) and the cyan antenna array for receiving (Rx), X dB is spatial beam isolation of 80-90 dB [13]

Furthermore, digital front end signal processing techniques should be applied to the SBFD transmitted signal followed by advanced signal processing techniques at Rx side in order to suppress Tx to Rx leakage and mitigate self-interference that are caused by the power amplifier non-linear behavior. So, in the next chapters, the power amplifier non-linear behavior followed by applied signal processing techniques at both Tx and Rx sides of the gNodeB, will be discussed in detail, where these signal processing techniques were the major focus that was worked on during this thesis in order to mitigate self-interference at gNodeBs.

In the end, Table1 below represents a conclusion comparison between duplex schemes.

Table1: Comparison of duplexing schemes FR1 [1]

	TDD	**FDD**	**SBFD**
Spectrum Efficiency	Better than FDD, coding techniques used via channel reciprocity.	Worse than TDD	Better than TDD, due to Tx/Rx operate simultaneously at the same time/frequency.
Latency	Worse than FDD, limited duty cycle	Low latency	Same as FDD
UL Coverage	Worse than FDD, UL limited transmissions	Excellent coverage	Same as FDD
DL/UL Resources Config.	Fixed and configurable DL/UL slots across cell	Spectrum allocated DL/UL	Fixed and configurable DL/UL sub-bands across cell
Interference	None	None	Reduced due to SI and CLI
Cross Operator Allocation	Strict DL/UL bias across operators	No bias needed	DL/UL alignment on fixed slots, Reduced CLI on dynamic slots
Suitable Networks	All types	All types	All types

3. Power Amplifier: Non-linearities & Correction Schemes

3.1. RF Power Amplifier

In wireless communications systems, the transmission is carried out using air interface over long distances. The transmission signals need to have a certain threshold power to propagate through long distances. RF Power Amplifier (PA) is the active electronic device that is used to increase the magnitude of power of modulated waves to a sufficient level which is required to reach the transmission distance. It converts the low-power signal into a high-power signal typically known as the power amplification of a signal. The input signal from the baseband is pre-processed, modulated, passed through a typical PA for amplification, and transferred to the transmitter antenna. On the receiver side, the received signal is amplified with the help of a Low-Noise-Amplifier (LNA) and then digitally processed to demodulate the signal. The purpose of the PAs is to provide sufficient power to the transmitting signal so that the received signal is strong enough on the receiver side to recover the original information. If the received signal is not received within the required power limit, the original information cannot be recovered, because a weak power level received signal shows a low Signal to Noise Ratio (SNR), which is the measure of the signal strength relative to noise. Low SNR shows that the noise level that is impacting the desired signal can result in data retransmission, which leads to increase Bit Error Rate (BER). Then, it will be hard to distinguish between signal and noise in decision region of demodulated signal constellation.

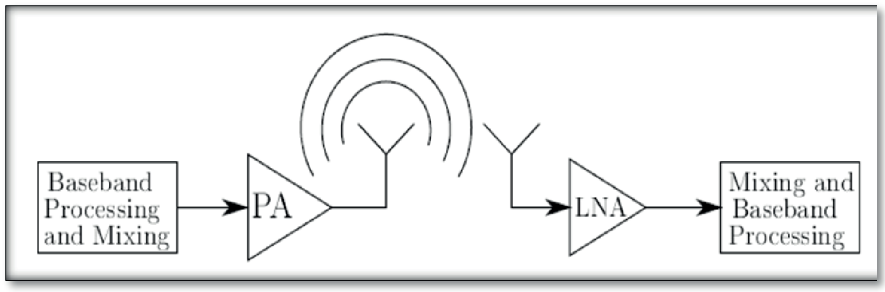

Fig. 3.1 Principle of communication system showing the position of PA on the transmitter side and the position of LNA on the receiver side [3]

Fig. 3.1 shows the position of a RF PA on the transmitter chain as the last active device which must handle the highest power in the RF chain. However, to achieve overall high system efficiency, the PA needs to be power efficient. The design considerations for a PA involved a trade-off between its efficiency and linearity. For the overall system efficiency, the PA needs to be efficient, and for the low distortion levels it needs to be linear.

3.1.1. Linearity of Power Amplifier:

The PA is used to increase the power level of an input signal without changing the contents of the signal. Fig. 3.2 shows a plot of input power versus output power of an amplifier which is a straight line representing a linear relationship of input power and output power. The gain is the slope of the straight line of the input power and the output power, for example, if the gain of an amplifier is 15 dB, then a 10 dBm input signal will result in a 150 dBm output signal. The straight line follows the linear relationship as seen in equation 3.1.

$$\text{Output Power} = \text{Input Power} + \text{Gain} \tag{3.1}$$

The amplifier shows this linear behavior to some input power level and then a point comes where output power starts saturating, then the relationship is no more linear where the straight line starts bending into a curve. The point where the gain decreases 1 dB from its constant value is called 1 dB compression point (P1dB) [4]. After this point, the amplifier enters in a non-linear region. The non-linear behavior causes many undesirable effects like distortions.

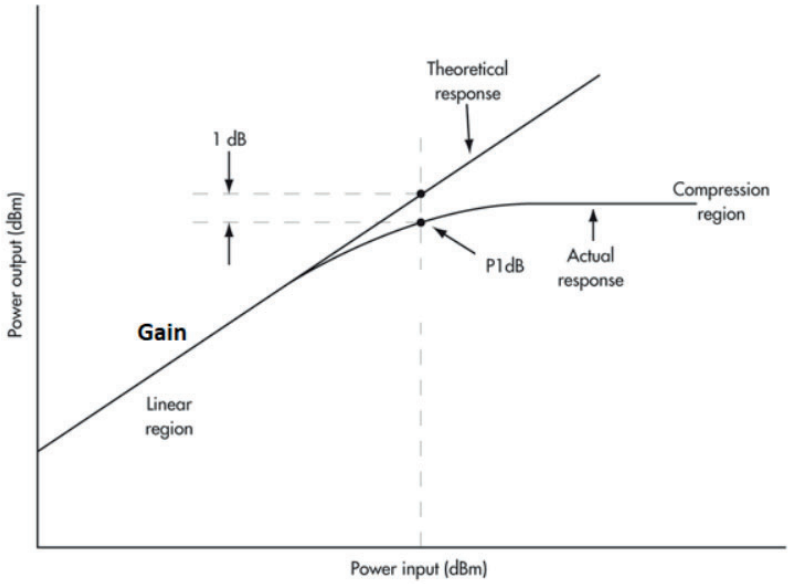

Fig. 3.2 Plot of Input Power vs Output Power of a power amplifier presents the P1dB, which is the point where the gain decreases 1 dB from its constant value [4]

3.1.2. Classification of Amplifiers

Amplifiers are categorized in two ways, one based on linearity and the other based on efficiency (switch mode). For Class A, Class AB, Class B, and Class C linear amplifiers are classed according to their construction and operating characteristics. When efficiency is more important than linearity, we consider Class D, Class F, and Class E amplifiers where the switch is used as an active device [5]. To understand the logic behind the trade-off between efficiency and linearity, it is necessary to study the classes of amplifiers.

Most of the time, a typical PA is operated on maximum output power for a fraction of time to achieve peak efficiency, which means it doesn't need to be efficient all the time during its operation because the input signal does not always contain peak amplitudes. A typical RF signal appears as sinewave over a short time interval while with a longer interval of time, the amplitude modulation is visible.

Even 50% efficiency for a Class A type PA is considered ideally satisfactory. The reason that the PA does not operate beyond acceptable

efficiency is the use of Orthogonal Frequency Division Multiplexing (OFDM) signal, which requires both amplitude and phase information to recover the signal at the receiver side. Overdriving the PA can increase the power efficiency, but it will introduce distortions for the amplitude and the phase of the signal by compressing the high-power levels in the signal [3].

3.1.3. Non-Linear System Effects

To understand the non-linear behavior of a PA on an input signal, it is important to study the distortion effects caused by a PA output. The amplitude and the phase of the OFDM signal both are affected by the PA. These properties are termed as Amplitude-to-Amplitude (AM/AM) conversion and Amplitude-to-Phase (AM/PM) conversion of the PA.

AM/AM characteristics of the PA show that when the input is applied, the output of the PA follows the linear region (straight line) but after some point on the line, the output starts saturating against any increment in its input power and shows a deviation curve from the linear straight line. As mentioned before in section 3.1.1, the point where the gain is dropped by 1 dB for any increment of input is known as the P1 dB compression point.

AM/PM characteristics of a PA show the unwanted deviation of the phase due to input amplitude causing a phase distortion. Both forms of distortions are presented in Fig. 3.3 (a) and (b).

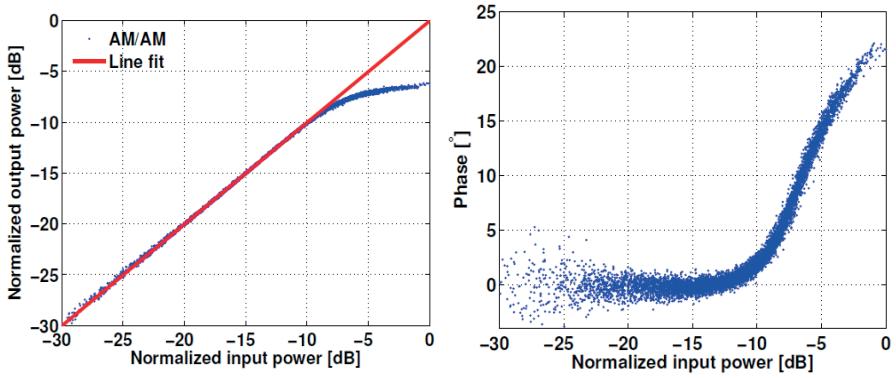

Fig. 3.3 (a) The graphical form of AM/AM shows the input signal appears to be linearly amplified with the normalized constant gain until a certain input power level. (b)The graphical form of AM/PM shows the distortion in the phase (degrees) of the output power as a function of the input power levels (dB) [3]

3.2. PA and Linearity Requirements

For an efficient use of a PA, it is very important for the PA to be operated in a linear region. In other words, at the high input power, the output should be linear under high efficiency. But, when the PA is operated at the maximum input power, the output starts saturating and the overall performance of the PA is non-efficient and causes non-linearity. The non-linear operation is responsible for the bad signal quality which leads to poor recovery of the transmitted signal and undesired interference.

3.2.1. Example of Non-Linear PA Test Case:

In Fig. 3.4(a), a 20MHz OFDM signal that has been passed through a non-linear region of a PA, the blue solid lines are the input of the transmitted signal, and the desired output is shown with dotted blue lines. The transmitter is operating in channel 0. The PA must amplify the main single strength within channel 0 but due to its non-linear effects, it shows the spectral regrowth represented by red dotted lines. This spectral regrowth can cause more serious problems like if the receiver in channel 1 can detect the signals at -76dBm/Hz and due to the leakage from channel 0 which interferes from -42dBm/Hz to -76 dBm/Hz, is not able to detect the signals in this range. This effect is well illustrated by Fig. 3.4 (a) below:

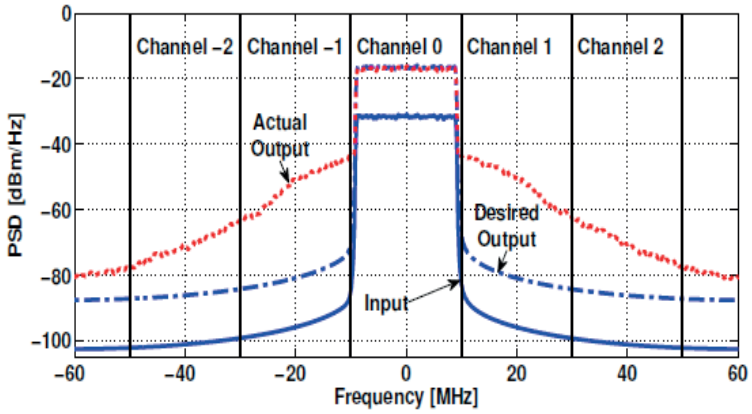

Fig. 3.4 (a) A transmitter is operating in channel 0, the desired output of the PA is shown with the dashed line, but the actual output of the PA shown with the dotted lines causes the spectral regrowth in the adjacent channels [3]

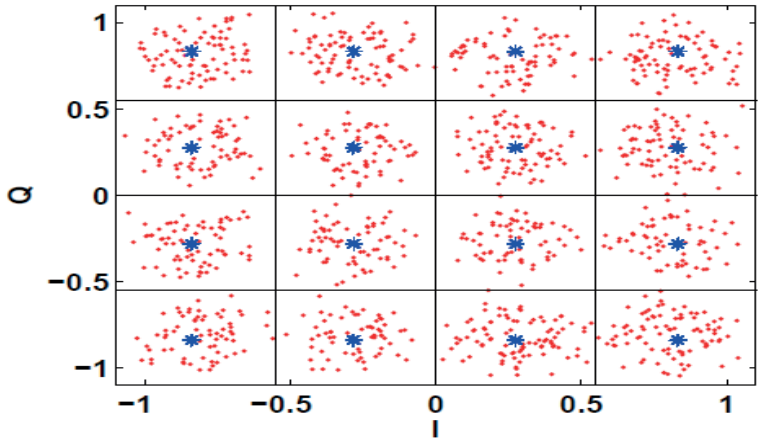

Fig. 3.4 (b) The red dots are demodulated 16-QAM data from the OFDM signal. The blue dots are the input signal showing a clear disturbance in the transmitted data [3]

In Fig. 3.4 (b), I/Q plot of the same received demodulated 20MHz OFDM signal which is presented in Fig 3.4 (a) is presented, the blue markers are the input signal data while the red dots are the demodulated data signal showing a massive distortion in the output leading to increment of BER.

3.2.2. Digital Correction of PA

Different techniques are used to improve a PA non-linearity depending on the signal to be amplified and the requirements of application. Linearity of the PA can be evaluated by some performance parameters such as Noise Power Ratio (NPR), the Adjacent-Channel Leakage Power Ratio (ACLR), and the Error Vector Magnitude (EVM). NPR is usually measured with Gaussian noise signals to determine the amount of noise created by amplification as a ratio of the desired output noise level. ACLR is a measure of how much energy is produced outside of a desired band, which could result in interference in multichannel communications systems. EVM is an evaluation of the amount of distortion in signal vectors, usually shown on a constellation diagram, typically specified in terms of peak and Root-Mean-Square (RMS) errors [3]. In this thesis, to evaluate the performance of SBFD scheme, we considered the ACLR and the EVM values when applying DSP techniques. For example, as will be seen in chapter 4, the ACLR between the

DL and the UL bands should be as much low as possible, and as will be discussed more in chapter 3, the EVM should not exceed 3%.

A PA can be corrected to exhibit the high linearity using several circuit approaches like the use of Digital Pre-Distortion (DPD). These approaches are utilized at the expense of efficiency and bandwidth. Also, there is a common practice of running a PA in a "back off" mode, which means that the PA will be operated only on an input power lower than the saturation point of the PA. Hence, sacrificing the efficiency with the reduced output power. To achieve the linear behaviour of a PA (currently it is operated in the backed-off mode which means the PA is not fully used as per its capabilities), there are many techniques to handle the non-linear behaviour of the PA used by industries depending on the complicities and the performances of their products [3].

3.3. DPD Technique

DPD is one of the popular techniques used by industries to improve the linearity of the PA to get optimal efficiency with low complexity. The DPD technique is greatly considered a correction method for RF PAs. The aim behind this is to reduce the power consumption of gNodeBs and UEs. Once the linearity of the PAs is achieved by the DPD, it can be possible to run it on a higher output power with lower distortion level, and a higher efficiency.

3.3.1. Basic Principle of DPD

Usually, the pre-distortion at the input of a PA is carried out in such a way that the distortion generated by a PA on the output side is compensated. This is done by calculating the inverse of the output distortion of the PA and sending it as feedback to the PA input. In Fig. 3.5, the basic principle of a DPD is shown. In the first step, the pre-distorter block generates the inverse of the input gain and combines it with the original input before passing through the PA. Combing input gain and pre-distorter gain, the final output is linear. The DPD works by calculating its estimation parameters. There are several learning architectures used to calculate these parameters.

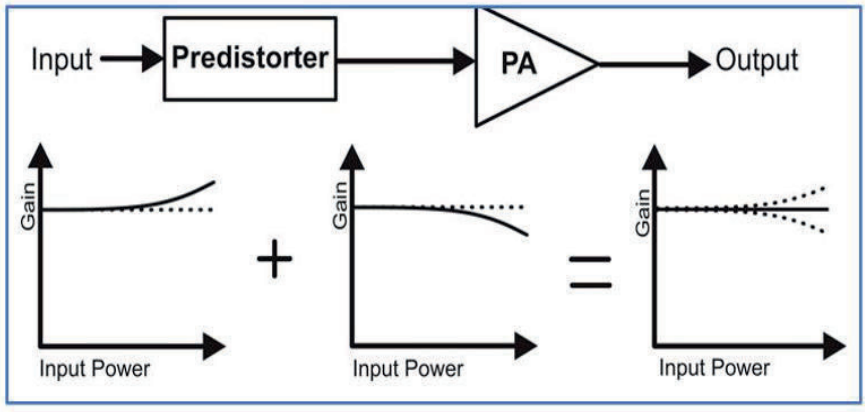

Fig. 3.5 Basic Principle of DPD [4]

3.3.2. Learning Architectures

To estimate the coefficients parameters of a digital pre-distorter, there are two different learning architectures methods namely Direct Learning Architecture (DLA) and Indirect Learning Architecture (ILA).

One important issue in the linearization of the PAs has always been that desired output values of the pre-distorter are unknown beforehand [3]. For this reason, digital pre-distorters are designed using either ILA or DLA. In this section we will briefly discuss both techniques and later, a new technique to design digital pre-distorters for the PAs based on ILC is presented [5].

3.3.3. System Blocks of DPD

The basic system blocks are presented in Fig 3.6 (a) where a pre-distortion function is calculated by a signal processing technique. There are three blocks for DPD implementation in the PA. The baseband signal is received at the DPD block, adjusted with some complex gain, and then sent to the Digital-to-Analog block where it is up-converted into an analog signal and entered through PA. The output of a PA is then sent back to the DPD block through the Analog-to-Digital block after down-sampling. Then, in the DPD block, the new adjustment in the pre-distortion function is calculated. See Fig. 3.6 (b).

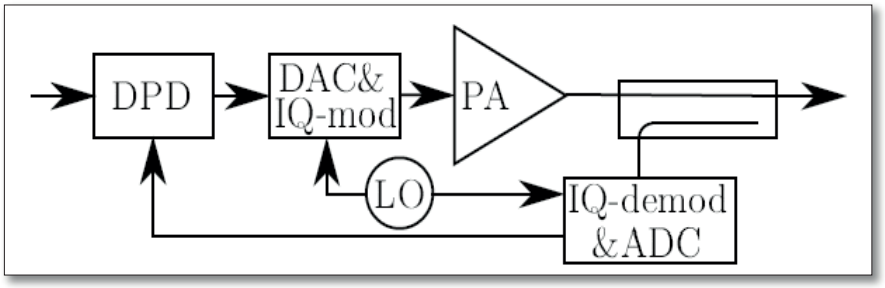

Fig. 3.6 (a) Block diagram of DPD and PA [3]

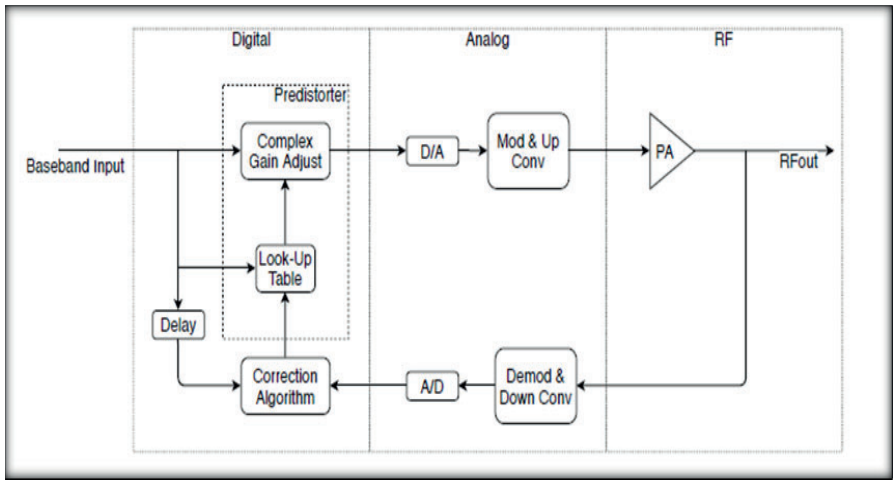

Fig. 3.6 (b) System block of DPD and PA [6]

The DPD block is designed to calculate pre-distortion based on received output from the PA, and then apply it to a new input to the PA. The new output is checked for any further adjustment of distortion level and repeats the adjustment for a few iterations until the correct inverse of the PA's output is obtained. On the other hand, Fig. 3.7 shows SBFD input and output signal with/without applying DPD block on the input SBFD signal, it can be observed that DPD technique is not enough to linearize the output of the PA, where out-of-band and in-band distortions are appeared.

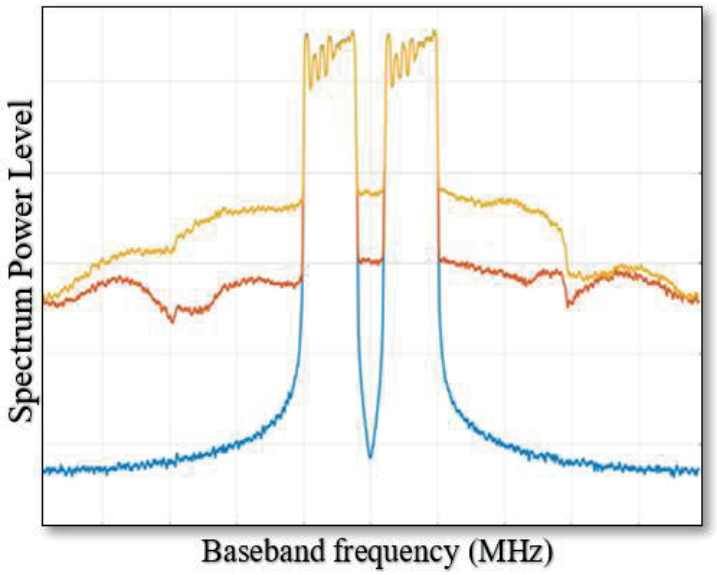

Fig. 3.7 SBFD Input signal (Blue), SBFD output signal without DPD (yellow), SBFD output signal with DPD (red). DPD supressed a little out of band distortions and in band distortions

One could consider that it should be enough to set filters on the output of the PA to remove in-band and out-of-band distortions. This can really be done but there are several reasons that prevent applying this approach, for example, the cost of such filters is expensive, filters do not provide flexibility to the new signals with new center frequency or bandwidth, and filters can cause even more in-band distortions [3].

On another hand, the efficiency of the PA is a function of the characteristics of the input signal, specifically in its Peak to Average Power Ratio (PAPR) or Crest Factor (CF), which are the ratio between powers or magnitudes related to the largest and the average power values of the signal, respectively. Furthermore, it is known that multi carrier signals, such as OFDM signals, show higher PAPR than single carrier systems. The reason behind that is the sum of multiple sub-carriers. In order to decrease unavoidable high PAPR in OFDM signals to linearize the PA behavior and achieve a higher PA efficiency, a previous signal processing algorithm to DPD is required. This algorithm deals with signals strive from unavoidable high PAPR or CF, while having constraints on how much the signal can be distorted, for example, EVM of input signal must not exceed a certain value [7].

The next sections explain in detail PAPR or Crest Factor Reduction (CFR) algorithms. But before going into these algorithms, performance parameters such as PAPR, EVM and ACLR is described in sections 3.4.1, 3.4.2, and 3.4.3.

3.4. CFR Algorithms

3.4.1. Definition of CF and PARP

CF is the ratio between the maximum magnitude value and the average value of a signal, observed in a certain temporal window, as shown in equation 3.2.

$$\mathrm{CF} = \frac{\|s(n)\|_{max}}{S_{rms}} \tag{3.2}$$

Where $||s(n)||$ is the peak amplitude and Srms is the rms value of the peak amplitude, and CF is the Crest factor.

We define the PAPR, again for a specific number of samples or a given interval of time, for discrete-time contexts, as shown in equations 3.3 and 3.4:

$$\mathrm{PAPR} = \frac{\|s(n)\|^2_{max}}{S^2_{rms}} \tag{3.3}$$

$$\mathrm{PAPR}_{dB} = 10\log_{10} \frac{\|s(n)\|^2_{max}}{S^2_{rms}} \tag{3.4}$$

From equations 3.2 and 3.3, it can be observed that PAPR= CF^2. The required influence of the various CF reduction algorithms is to reduce the PAPR of the signal without inserting too much distortion. Some of the algorithms will not insert any distortion at all, with the cost of a higher complexity and/or reduction of data rate, whereas some other will insert unavoidable distortions both in-band and out-of-band. Both in-band and out-of-band are indeed objectionable and to evaluate them, two parameters exist: EVM, and ACLR.

3.4.2. Definition of EVM

EVM is an evaluation of the displacements of the received output signal compared to the input ideal signal. Such displacements that can distort the input ideal signals are noise and, as in our thesis, the CFR interception. The EVM is expressed in dB, but most commonly the EVM is used in percentage in most of the performance models. We define it as (see Fig 3.8):

$$\mathrm{EVM_{dB}} = 10\log_{10}\frac{\mathrm{P_{error}}}{\mathrm{P_{ref}}} \tag{3.5}$$

$$\mathrm{EVM}(\%) = \sqrt{\frac{P_{error}}{P_{ref}}}.100 \tag{3.6}$$

Where $\mathrm{P_{error}}$ is the sum of all the error vector powers and $\mathrm{P_{ref}}$ is the sum of all the reference, expected, signal powers. As shown in Fig 3.8, the error vector is the vector in the I/Q plane that binds the received symbol with the ideal position matching the exact transmitted symbol. For each received symbol, the corresponding power is calculated and averaged, then divided by a correctly chosen value delegate for the modulation scheme (EVM normalization reference). The result is an accumulate measure of how much the whole transmitter-receiver chain is adjacent to the ideal from the precision standpoint [7].

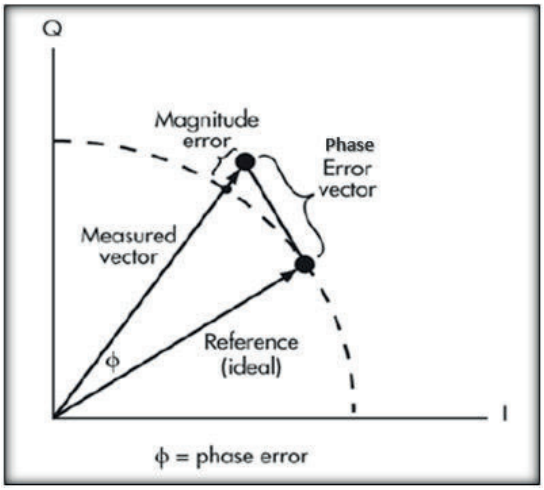

Fig. 3.8 The reference (transmitted) and the measured (received) vectors are presented on the I-Q plane. The power of the error and the reference vectors are used to compute the EVM [7]

In this thesis, in-band distortion introduced by the CFR algorithm has an apparent influence on the EVM which is considered as a measurement of the performance of the CFR method (will be explained in the next chapter).

3.4.3. Definition of ACLR

As shown in equation 3.7, ACLR is defined as the ratio of the power leaked to the adjacent channel and the power in the main channels (see Fig. 3.9) [7].

$$\text{ACLR} = \frac{\text{Adjacent Channel Power}}{\text{Main Channel Power}} \tag{3.7}$$

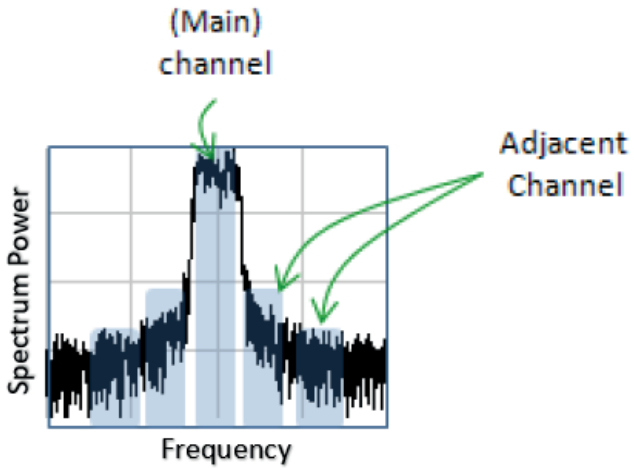

Fig. 3.9 ACLR components [7]

ACLR is a measurement referring to evaluate out-of-band distortions. As shown in Fig. 3.9, the ACLR level must be very low to mitigate interference in the neighbouring channels. Moreover, a high ACLR translates to some main channel energy wasted over adjacent channels therefore cutting down the efficiency of the transmission. For example, in Fig. 3.10, a high ACLR value in the middle band can be seen, which shows in-band distortion. Besides, with this value of ACLR, a simultaneous transmission and reception in SBFD scheme cannot be obtained, where the UL transmitted signal will interfere with middle band signal that shows in-band distortion.

CFR Methods

There are several methods that have been proposed to mitigate the PAPR problem in input signals [5]. Two of the methods are tested in this thesis:

1. Clipping and Filtering (CAF)

2. Peak Cancellation (it will be discussed in detail in the next chapter)

3.4.4. CAF Technique

CAF technique is the simplest method available and based on limiting the detected peak amplitude to a certain level, this level is configured by an appropriate threshold value. Multiple methods are proposed on how this limiting is implemented [5]. In this thesis, we used a hard clipping where all inputs samples magnitudes higher than the threshold value (the desired maximum value for the magnitude of the input signal) is specified to be equal to threshold value level, where the threshold value level can be selected depending on the maintained value of the EVM [5]. Besides, as the clipping is a nonlinear operation which generates out-of-band distortions, the clipped input signal samples must be filtered to reduce the out-of-band distortions and reach acceptable ACLR levels in the frequency domain. Filtering generally makes some of the peaks retrieved in the time domain because hard clipping is a nonlinear operation that spreads the signal in the frequency domain, like spectral regrowth from a PA. When this spreading is reduced by a filtering, the signal in the time domain is partially restored, which means the peaks appear again in the time domain [7].

In addition, as a test for the CAF technique, the hard clipping and filtering technique is applied recursively on a single SBFD signal followed by the DPD technique to mitigate the spectral regrowth produced by the PA. The iterative CAF technique is called Turbo Clipping (TC) and developed by Ericsson.

Fig. 3.10 shows Ericsson implementation of a PA output preceded by CAF and DPD applied techniques on a single SBFD input signal. The bandwidth of the input SBFD signal is 60 MHz (20 MHz DL, 20 MHz UL, 20 MHz DL). With 3% EVM, PAPR decreased from 9.3 dB to 7.9 dB. The out-of-band distortion is cancelled, but the output signal still has in-band distortion caused by the hard clipping, where a high ACLR can be seen. This in-band distortion should be reduced as much as possible, to mitigate crosslink interference and self-interference at gNodeBs and to ensure simultaneous transmission and reception at gNodeBs.

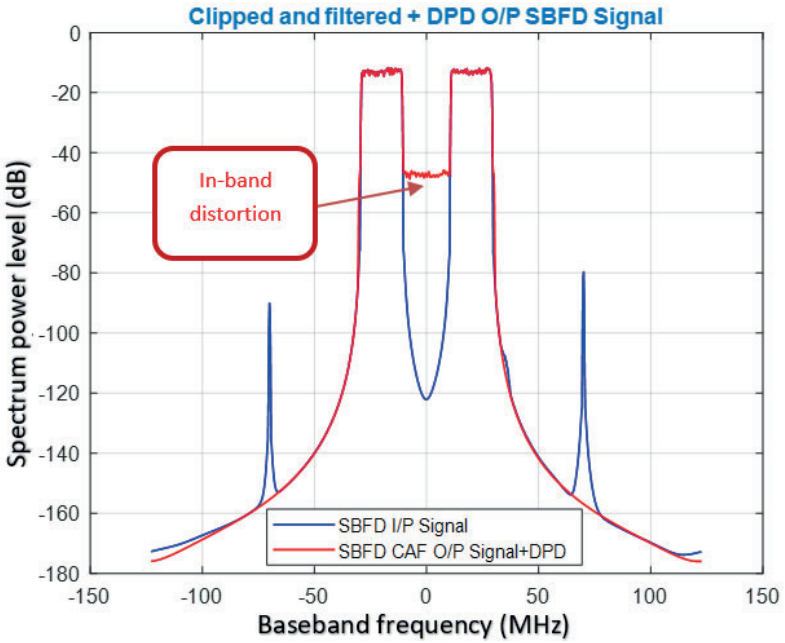

Fig. 3.10 PA output preceded by CAF/Turbo and DPD applied on a single SBFD input signal (Y-axis represents spectrum power level in dB, X-axis represents baseband frequency in MHz)

As shown in Fig. 3.10, in the SBFD signal, the in-band distortions must be cancelled along with the out-of-band distortions. So, we decided to use a Peak Cancellation (PC) technique instead of CAF/TC. In the PC technique, the transmitted signal that contains peaks with high power levels in comparison to the average power is shaped into a signal that contains a lower peak power level while the average power is maintained, while having constraints on how much the original signal is distorted, for example, the EVM should not exceed 3% after shaping the signal.

The major advantage of PC technique is complexity reduction of the algorithm compared to CAF technique because of the absence of actual filtering after clipping error. Then, it can be observed that the PC technique is less expensive compared to CAF technique because there is no need for physical expensive filters [5].

The next chapter (Peak Cancellation Crest Factor Reduction) describes in detail a PC algorithm, which was one of the major algorithms that we worked on during our thesis journey.

4. Peak Cancellation Crest Factor Reduction (PC-CFR)

4.1. General Description of PC-CFR Algorithm

As mentioned in section 3.3.3, the PC-CFR module is usually placed after combining all the signals coming from different channels and before the DPD, as seen in Fig. 4.1.

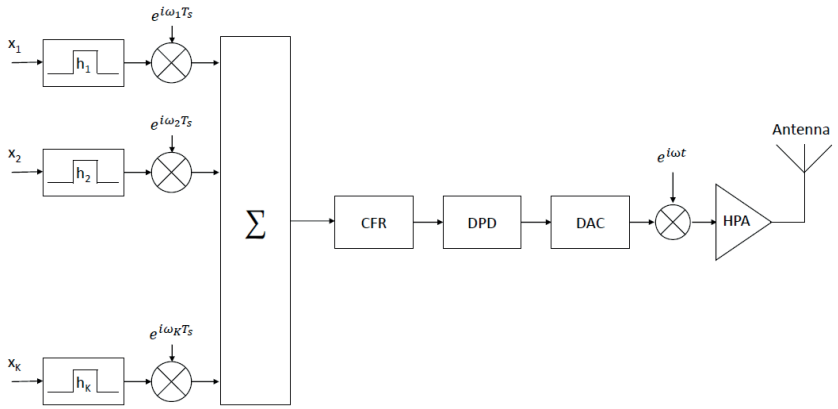

Fig. 4.1 CFR position inside the communication Chain [7]

The purpose of the PC-CFR is to reduce the PAPR of the input signal to a required value of PAPR and maximum value of EVM. The input signal to the PC-CFR block is made of in-phase and quadrature parts (complex signal), it is the sum of all various components relative to the various carriers. The result is a high PAPR discrete time signal. The output from PC-CFR is a reduced PAPR and delayed signal with the same format.

In the PC-CFR block, the threshold value of the peaks is set to a value that is related to the target PAPR [7]. When the input signal is greater than the threshold to meet the target PAPR, the peak is detected and then the peak is scaled by subtracting the threshold value from the amplitude of the detected peak as shown in equation 4.1.

$$\text{Peak scale} = \text{Maximum detected Magnitude} - \text{threshold} \qquad (4.1)$$

The PC-CFR algorithm implements a time-domain signal processing on fixed and picked samples of the input signal. Such samples are detected

depending on appearance of the peaks which can be defined as follows: given the range of samples of the input signal starting from the first sample peak that has a magnitude greater than the threshold and finishing after a specific number of samples, the peak is the element having the maximum magnitude inside this interval. A conversion from rectangular to polar format to expose the magnitude of the input samples is required as one of the first steps of the algorithm, because the detection of the peaks is made based on the magnitude of the input samples. For each detected peak, a cancelling pulse is generated and then subtracted from the input signal to reduce the value of the peak to the value of the threshold.

The complex coefficients (magnitude and phase) of the cancelling pulse are extracted from a designed filter that has the same shape as the input signal in frequency spectrum and stored in a memory; these coefficients are the same for each peak being cancelled. The cancelling pulses are generated by a simple complex multiplication between each of the coefficients of the stored unscaled cancelling pulse, and a single complex number coming from the peak detection and scaling part of the algorithm, this process being implemented for each peak separately.

The parts of the peak **P** that are required for the generation of the cancelling pulse are:

The scaled value (**ps**): the difference between the magnitude of the sample selected as peak (**Sk**, for some k) and the threshold.

The phase.

$$\mathbf{P} = \mathrm{ps} \cdot e^{j\theta \mathrm{ps}} \; ; \; \mathrm{ps} = |\mathrm{Sk}| - \mathrm{threshold} \tag{4.2}$$

The cancelling pulse elements **c[n]**, are generated according to equation 4.3:

$$\mathrm{c[n]} = \mathrm{ps} \cdot \mathrm{s[n]} \cdot e^{j(\theta \mathrm{ps})} \cdot e^{j(\theta[\mathrm{n}])} \tag{4.3}$$

Where $\mathrm{s[n]} \cdot e^{j\theta[\mathrm{n}]}$ are the coefficients of the unscaled cancelling pulse for all the values n.

At the output of the multiplier, the complex data is converted back to the rectangular form, to make it ready to be subtracted from the delayed input signal, thus finally cancelling the peaks.

It should be observed that this algorithm requires a much less amount of hardware resources than other filtering-based CFR signal processing algorithms, where physical filters are used after clipping errors [3] [7].

It may certainly occur that more than one cancelling pulse needs to be generated simultaneously, so that coefficients of their intervals interfere. To provide the accumulating effect of all the cancelling pulses, all the coefficients of the active pulses must be added together and then subtracted from the delayed input signal at each sample of interest. Another observation is that the cancelling pulse successfully cancels only the peak element, where the central element of the unscaled cancelling pulse (which extracted from a designed filter that has the same shape as the input signal in frequency domain) is the actual element that, when multiplied by the detected peak coefficients, and subtracted from the delayed input signal, will give as a result an element with precisely equaling magnitude to the threshold value. These sequential steps are explained in section 4.2.

Fig. 4.2 shows the effect of the subtraction and the subsequent reduction of the peak to a magnitude matching the threshold on the complex plane. For example, the blue row which has magnitude higher than the threshold value, which is shown in the red circle, can be scaled to the black dot value, which is equal the threshold value, and it can be observed that the phase of the blue row peak is preserved as it is. Furthermore, All the neighbor input samples will be adjusted, as already explained above, in such a way that their magnitude will be reduced, but it should be noticed that the algorithm has not precise control over these elements, therefore some unacceptable occurrences are unpreventable, as it will be illustrated shortly.

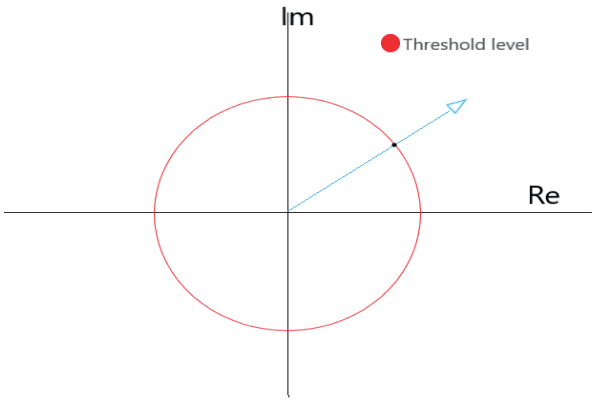

Fig. 4.2 Reduction of a complex sample to a version with the same phase and magnitude equal to the configured threshold, where the blue row is reduced to the black dot level that is on the red circle which represents the threshold level

In order to achieve a better result, the PC-CFR algorithm is usually applied more than once to the signal, and this can be done by making the output of the algorithm that is calculated in a certain stage, becomes the input of the next stage in a cascaded PC structure as shown in Fig. 4.3. The reasons for which this is usually done are discussed in the following sections 4.1.1, 4.1.2, and 4.1.3.

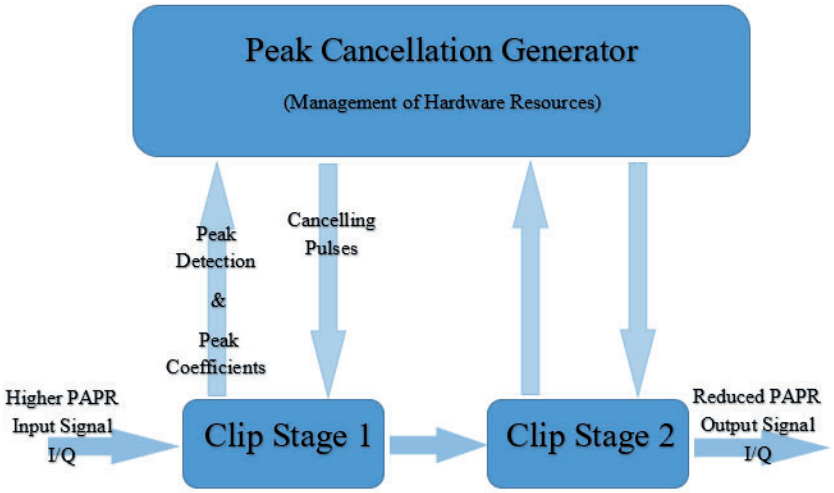

Fig. 4.3 Example of architecture of the PC-CFR module, with two cascaded Clip Stages

4.1.1. Peak Leak

If an implementation of the PC-CFR algorithm constitutes a maximum limit of the number of simultaneous cancelling pulses that can be generated by a single stage, then it occurs that, when such limit is attained and a new peak is detected, the peak will be passed uncancelled through the stage, which is the case we battle to avoid in the first place. By cascading multiple stages, the probability of the peak leak will be decreased. The parameters that may affect the peak leak scenario are presence, density, and magnitude of the peaks. Based on these parameters, we can identify how many Clip Stages (CSs) should be applied in the PC-CFR structure [7]. For example, if for a specific value of the threshold no peaks are detected, it may be possible that

for a lower threshold, the same combinations of input values show one or more peaks.

The length of the Peak Search Window (PSW) (i.e., how many samples are detected in search for the peak) can also affect the number of closely spaced detected peaks. The same set of input elements could give a larger or smaller number of detected peaks depending on the length of such interval. The longer the interval yields to fewer detected peaks, because larger number of samples will be associated with single peaks.

4.1.2. Peak Regrowth

The subtraction of the cancelling pulses from the input signal covers a much larger number of samples than the peak alone, a constructive summation may be occurred for the samples that they were smaller than the threshold before the cancellation of a peak, and the samples maybe raised over threshold after the cancellation of a peak, thus becoming peaks themselves. Although they were not in the beginning and provoking the event called peak regrowth. It can be noticed that the magnitude of the regrown peaks is correlated with the height of the original cancelled peak, with recognizing that with the greater peak, the probability of appearing regrown peaks is increased after its cancellation. By cascading multiple stages, the peak regrowth event can be under control as well.

4.1.3. Gradual Peak Reduction

It may occur that one or more peaks are not completely cancelled while more cancelling pulses operate simultaneously in an interval, because of the reciprocal interactions among cancelling pulses. This event has a high probability of occurring, unavoidable and its effects are tougher in case of greater peak to cancel.

To attenuate this and the effect of the peak regrowth case, an intelligent way consists of gradually decreasing the magnitude of the peaks by putting progressively decreasing thresholds in consecutive stages of the PC-CFR, instead of attempting to completely cancel them in one pass. This can be distinctly fulfilled by a cascading architecture because each iteration of the PC-CFR may be separately configured with a distinct set of parameters, such as the threshold.

Performing multiple CSs requires higher power consumption and introduces a higher delay on the signal, which in general is an unfavorable outcome especially for the more recent communication protocols. The delay in the signal data path is introduced to compensate for the time consumed to

execute all the computations representing the algorithm. The largest fraction of the delay is by far the group delay of the cancelling pulse itself, which clearly cannot start before the actual detection of the peak.

It can be observed that this algorithm includes some signal processing which in turn will change the characteristics of the input signal thus bringing up both in-band and out of band distortion. To decrease this unwanted consequence, the unscaled cancelling pulse is designed so that its frequency spectrum will match that of the input signal as mentioned before.

The number, bandwidth, and relative positions of the carriers constitute the spectrum of the input signal. Thus, a longer cancelling pulse represents more coefficients it is made of, then subtraction cancelling pulses from the input signal produces tougher effect on the input signal because the process will affect a larger number of coefficients, influencing negatively on the EVM; also, larger memories are required in case of longer cancelling pulses which will create longer delays.

On the other hand, as mentioned in section 3.4.4, the PC-CFR strategy has a prominent advantage over the TC and other filter-based algorithms, which is its flexibility in case of changes of the input signal characteristics. In fact, PC-CFR algorithm adapt to a different configuration of the input signal carriers, it is just an order of changing the coefficients of the unscaled cancelling pulse by a re-configuration of the pulse memory, thus reinforcing the advantage of the module for several cases. The TC algorithm, alternately, operates on each carrier separately via a designed branch including one or more decimators, Finite Impulse Response (FIR) filters, and interpolators. It follows that the total hardware architecture of the TC is formed upon a special configuration for the input signal carriers, and it cannot be reconfigured easily. In TC, the per carrier filtering permits a more precise and so, effective interference on the input signal, whereas the cancelling pulse in the PC-CFR is configurated depending on the characteristics of the input signal carrier configuration and therefore is sub-optimal with respect to each carrier [7].

4.2. Implementation Structural Description

The PC algorithm architecture is made by a determined number of cascaded CSs, as shown in Fig. 4.3. Each of them connecting with a centralized controlling module called Peak Manager (PM). The cascading set of CSs composes the data path of the signal and lets the iteration of the algorithm be applied with the required number of CSs. The proposed PC algorithm is flexible, for example, every CS can be configured with a specific threshold and PSW length. In each CS, consecutive operations are performed:

conversion from rectangular to polar form of the input signal, peak detection, sending to the PM the detected peak coefficients (Amplitude and Phase), creation of the unscaled cancelling pulses, complex multiplication with the detected peaks, the conversion from polar to rectangular to apply subtraction from the delayed input signal.

The PM receives notifications about the coefficients of the detected peaks from all the connected CSs, and then generates and sends the cancelling pulses off to them if at least a Peak Cancelling Unit (PCU) is available. PCU is the set of hardware and physical resources (time slot in the Time-Division Multiplexing rotation) needed for the generation of a cancelling pulses.

The PM handles multiple tasks: store the coefficients of the unscaled cancelling pulse in its memory, complex multiplication, conversion of the data from the polar back to the rectangular form and subtraction from the delayed input signal to combine all the cancelling pulses before sending them to the next CS. Furthermore, a controlling unit and a pulse generator should be existed to perform the overall management of the whole PC algorithm.

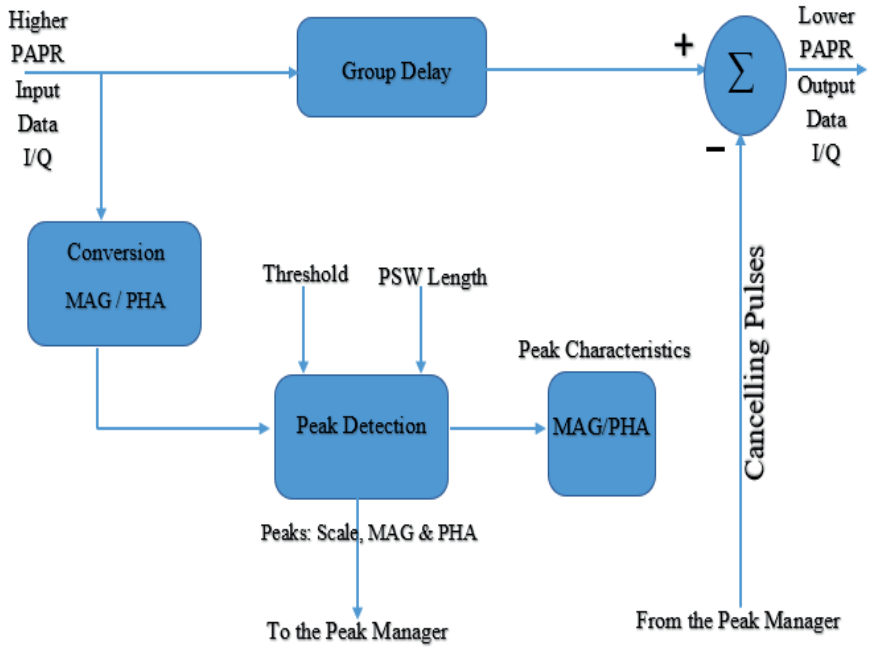

Fig. 4.4 clipping stage block diagram [7]

4.2.1. Consecutive CSs

Each CS receives the input signal from the output of the previous CS in the form of I/Q signal samples, where the output represents the difference between the delayed input signal and the cancelling pulse, as seen in Fig. 4.4.

The first step in each clipping stage is the conversion of the input complex signal sample from rectangular to polar form, so that the magnitude of each signal sample is revealed, and the peaks can be detected.

At that moment, each sample is transferred to the second step which is called peak detection. At peak detection, the status remains in IDLE state until a sample exceeds the threshold value. Then the peak detector moves to the *Peak Search* state where successive samples are compared to the last maximum detected sample in the PSW to find the maximum magnitude sample within the whole interval. This is implemented by comparing the magnitude of each new input sample with the maximum detected sample which is stored in a register with the corresponding phase. Then, the threshold value is subtracted from the maximum input sample magnitude found in the PSW; this process is called *peak scale*. At the end, the peak detector sends the peak scale, subtracted sample signal and the relative phase to the PM, and updates the peak statistics as shown below in Fig. 4.5.

The threshold of the peaks should be configured in the peak detector to recognize the final desired PAPR. The PSW length should be configured as well, to determine how many samples are observed in each search of the peaks. Both threshold and PSW can be adjusted independently for each CS.

In the implementation of the peak detector, a peak detector table is constructed by MATLAB that includes the detected peak statistics which are: peak index, peak scale, peak phase, and other variables that will be mentioned in the next sections for better understanding.

4.2.2. Group Delay

As shown in Fig. 4.4, the input signal is delayed for compensating the delays by the other processes handled by CS and PM. In our PC structure, we adopted the amount of the group delay to be half the number of the filter coefficients in the PM as recommended in the most of research papers [7].

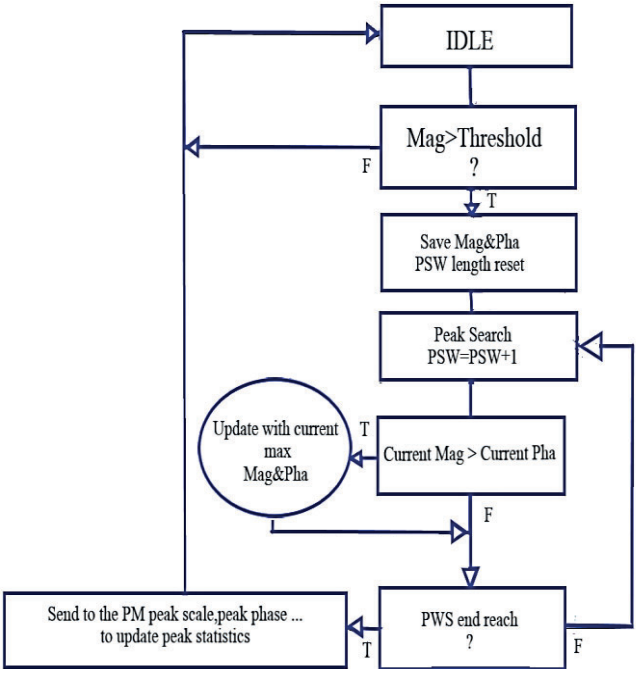

Fig. 4.5 Peak detection adopted algorithm [7]

4.2.3. Ultimate step subtractor

As a decisive step, the cancelling pulses that come from the PM are subtracted from the input delayed signal. In this step, we have delay per CS, but we do not have to compensate it by the group delay because it is the ultimate process applied to the signal.

4.2.4. The PM Unit

The PM is a centralized unit that receives the detected peaks from all the CSs, generates appropriately the cancelling pulses, and returns them to the current CS to cancel the detected peaks.

The PM uses the PCUs to manage the unscaled cancelling pulses. The PCU stores the unscaled cancelling pulses and generates them depending on the detected peaks table constructed by the peak detector. The unscaled cancelling pulses should be matched with the peak detector table to generate the corresponding coefficients for each detected peak. An address generator

is used to determine the unscaled cancelling pulses start and end indexes addresses.

In the PM, a digital filter is implemented with an identical output of the input signal spectrum. The coefficient of the digital filter is extracted to be the unscaled cancelling pulses for the detected peaks. In this project, we adopted the order of the digital filter to be 1024. So, we extracted 1024 coefficients to be the cancelling pulses that should be generated by the PM, where with 1024 digital filter order we get the best PC results. Fig. 4.6 below shows the spectrum of the implemented digital filter.

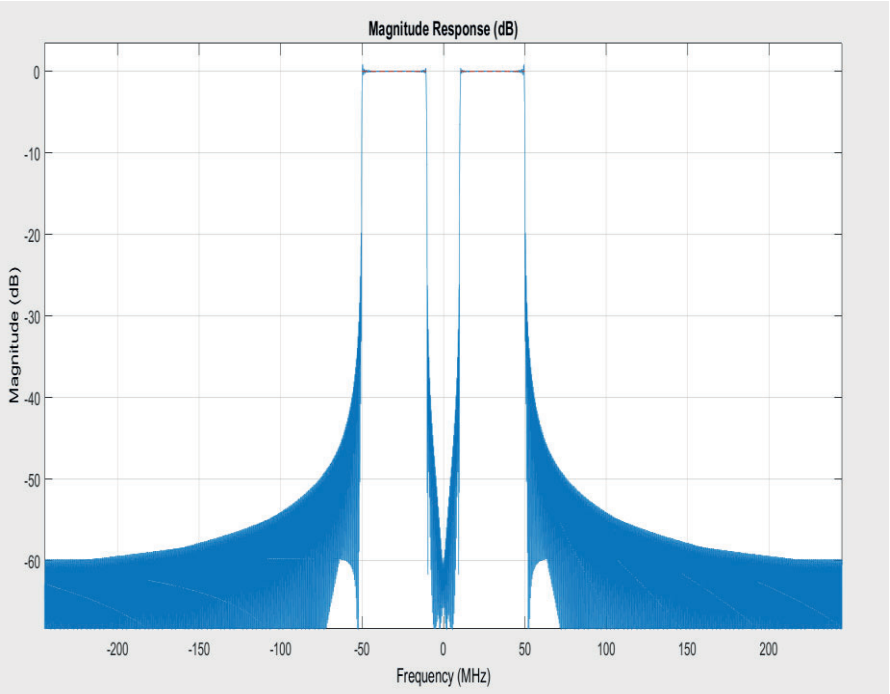

Fig. 4.6 Magnitude response of the PM digital filter

It can be noticed; the impulse response of the digital filter is symmetric with response to the central coefficient as shown in Fig. 4.7. With this symmetric property, saving half of the digital filter coefficients would be possible, thus implementing a smaller memory in the PM. On the other hand, we should take into consideration that the phase is not symmetric, so in case that the central value 511 has been reached over a total of 1023 coefficients, the counting direction should be inverted.

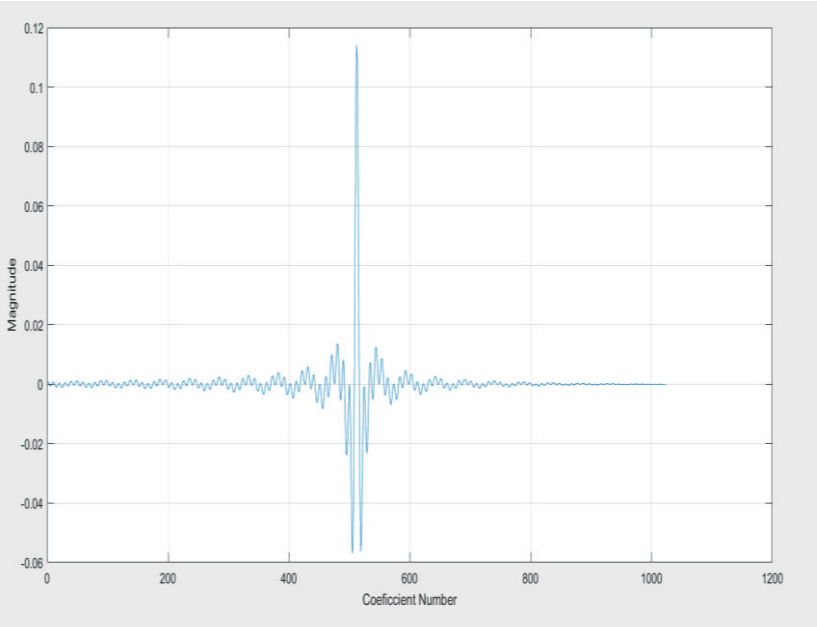

Fig. 4.7 Magnitude of the unscaled cancelling pulse before multiplication with the detected peak coefficients

The address generators get the start address of each unscaled cancelling peak from the peak detector table. The start address depends on the peak scale value, where the energy of cancelling pulse with higher detected peaks is larger compared to the smaller detected peaks. That is because the cancelling pulse is the multiplication of the detected peak scale and the unscaled cancelling pulse, thus cancelling pulses with higher detected peaks are larger in magnitude and in energy as well. So, it is observed that multiplying low detected peak scale with small coefficients magnitude has extremely negligible effect on the detected peaks. Thus, it is possible to use shorter cancelling pulses to cancel smaller detected peaks, then the start address of the unscaled cancelling pulses can be assigned to be larger than zero, depending on the detected peak height. For example, we mapped the value of 450 to be the start address of unscaled cancelling pulse in case that the peak scale is around 0.01, depending on scanning of the detected peaks of our signal and reading the peak scale values for every detected peak, a perfect mapping of our signal occurred where the start address of the unscaled pulses is chosen where the pulse passing through a zero or at extremely low magnitude to decrease the discontinuities and out of band distortions. Table

4.1 below shows some detected peaks with its index, scale, phase, and starting address of unscaled cancelling pulse.

Table 4.1 Peak information table sample: The whole pulse coefficients are multiplied by the detected peak scale in case that the scale is high, and the start address is 1, and vice versa

Index	Scale	Phase	Starting address of unscaled CP
25	0.02546	1.2364104	200
559	0.00087	1.8928676	450
657	0.02171	1.1186577	300
929	0.00591	-2.330755	450
1035	0.02260	-1.410903	300
1104	0.08149	1.9541709	1
1407	0.00070	0.6843572	450

As for further improvement to our PC-CFR structure, the number of PCUs for each CS is increased to improve the output of the PC-CFR structure, where N PCUs requires N memories to store the coefficients of the unscaled cancelling pulses for all the detected peaks, where they are same for each detected peak as mentioned before. This will lead to an increase in the number of cancelled peaks during each CS and decrease the delay at the PM. For example, in our MATLAB implementation we used eight, four, four, and two PCUs for each operation, respectively. Where with this configuration the PAPR is decreased as much as possible with 3% EVM. For example, for a single SBFD signal with 40 DL, 20 UL, 40 DL MHz the PC-CFR structure is applied as shown in Fig. 4.8, and we got a decrease of PAPR from 9.2dB to 8.6dB with 3% EVM. The targeted PAPR was 6dB configured by the threshold value of the peaks. The threshold value could be configured separately for each CS, but in our implementation, we used just one threshold for all four CSs as shown in Fig. 4.9.

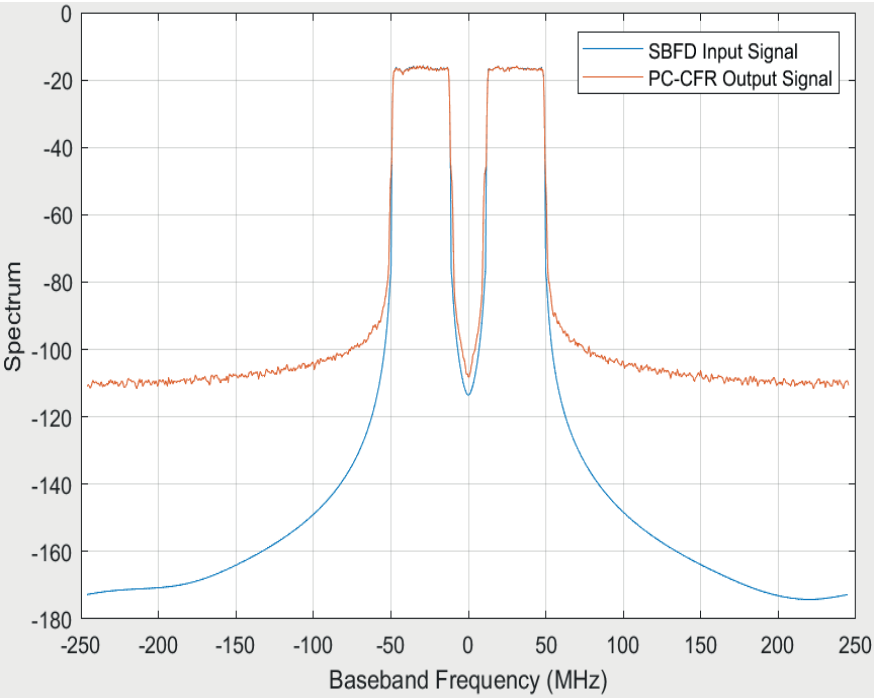

Fig. 4.8 PC-CFR applied to a single SBFD signal

From Fig. 4.8 and Fig 4.9, we can observe that the PC-CFR process has been completely succeed, where both out of band and in band distortions have been eliminated. As we mentioned before in section 2.4.4, the next step will be applying a DPD technique on the input signal to decrease the nonlinearity behavior of the power amplifier.

At that moment, we decided to apply PC-CFR followed by DPD on 32 branches SBFD input signals as will be shown in the next chapter. Besides, to suppress more the UL band distortion and mitigate self-interference at gNodeBs, an advance digital signal processing technique called Self Interference Cancellation (SIC) is applied on the SBFD UL band signal at the gNodeB receiver side. SIC will be explained in detail with showing design methodology and results of 32 branches SBFD input signals transmission and receiving scenario at gNodeB in the next chapter.

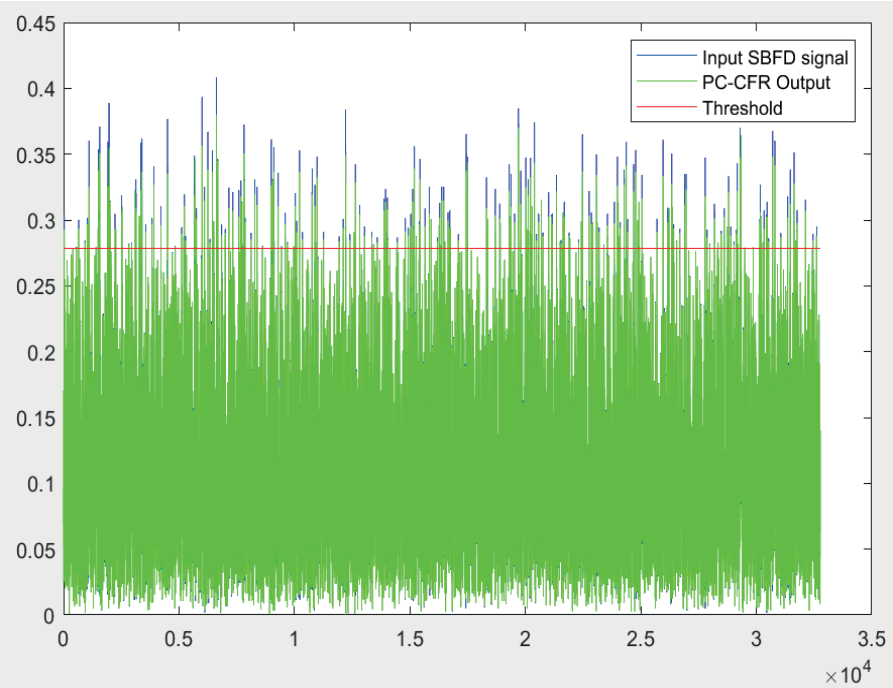

Fig. 4.9 Input SBFD signal and PC-CFR output

5. Design Methodology and Results

As mentioned before, power amplifier at transmitter introduces a non-linear behavior that generates distortions and spectral regrowth. These distortions must be sampled at the output of the transmitter, and digital front end signal processing techniques must be applied on the transmitted signal to eliminate these distortions. At the end, SIC solution must detect and compensate for real-time changes caused by temperature variations, mechanical vibrations, or the motion of things in the environment [8]. According to Wikipedia in [11], "SIC is a signal processing technique that enables a radio transceiver to simultaneously transmit and receive on a single channel, a pair of partially overlapping channels, or any pair of channels in the same frequency band". SIC sometimes defined as “in-band full-duplex” or “simultaneous transmit and receive” when it is used to permit simultaneous transmission and reception on the same frequency [11]. In SBFD communication scenario, we used SIC in order to suppress more the UL band in SBFD signal and reducing leakage from Tx channel to Rx channel at gNodeB side and, consequently, reducing SI at gNodeBs.

As shown in Fig. 5.1, which shows SIC technique block diagram, the UL band in SBFD signal can be suppressed more by filtering out the UL band signal digitally, and then using it to generate SIC output signal, where the filtered UL band signal combined with the signals arriving at the receiver and the receiver noise to leave only the desired receive signal (SIC O/P). The exact amount of cancellation can vary depending on the power of the UL band transmit signal which represents the source of the self-interference, and the signal-to-noise ratio (SNR) that the link is expected to handle in full-duplex mode.

In addition, as shown in Fig. 5.1, cancelling a local transmit signal requires a combination of analog and digital electronics, where the strength of the transmit signal can be reduced before it reaches the receiver by using Radio Frequency (RF) canceller. RF canceller can be designed using a circulator, or antenna isolation techniques if separate antennas are used. Besides, RF canceller could be an analog or a digital canceller, both the analog and digital cancellers include several “taps” consisted of attenuators, phase shifters, and delay elements. Besides, the tuning algorithms are necessary to enable the canceller to adapt to rapid changes in the environment [9][10].

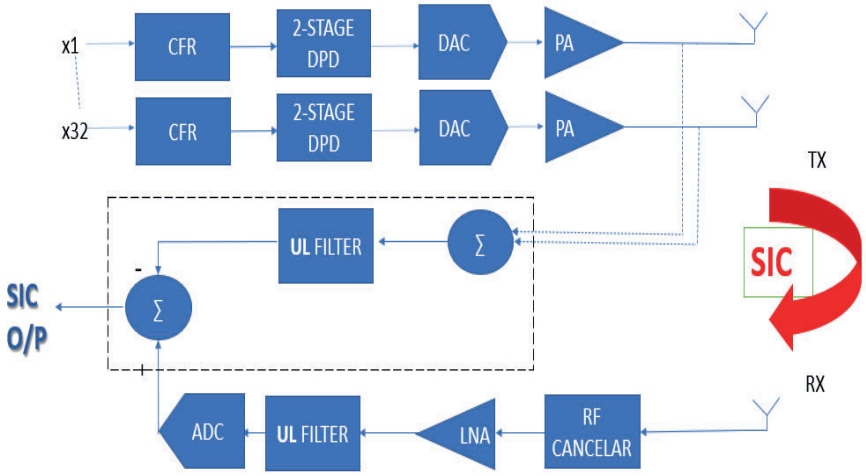

Fig. 5.1. SIC block diagram, combination of filtered UL band with receiver signals (UL band signal, UE signal or 'interfered signal' and receiver noise)

In this thesis, we used a digital RF canceller to reduce the average power of the transmitted SBFD UL band. Different RF cancellation levels are applied on the SBFD UL band signal (from 0dB to 20dB) to evaluate the performance of SIC technique with different required SNR levels (from 5dB to 20dB), as will be discussed in the implementation and results section.

5.1. Implementation and Results

As mentioned before, in order to eliminate the nonlinear behavior of the power amplifier and reduce self-interference between Tx channel (DL bands) and Rx channel (UL band) in SBFD scheme, and then to provide simultaneous transmitting and receiving at gNodeBs, one of the key enablers is applying DFE signal processing techniques (PC-CFR and DPD) at transmitter side of gNodeB followed by an advance signal processing technique (SIC) at receiver side of gNodeB as shown in Fig. 5.1.

Fig. 5.2 shows 32 branches SBFD input signals, as a first stage they are passed through the PC-CFR blocks, where PARP of 32 SBFD input signals is reduced in the way that is described in the chapter of PC-CFR before. PC-CFR technique is applied separately on each SBFD input signal branch, and a tradeoff between PAPR and EVM is considered, where the PAPR is decreased for each SBFD signal branch depending on an approximately 3% EVM value for each peak cancelled in each SBFD input signal branch. Then the 32 SBFD signals are passed through DPD blocks along with the PA. Moreover, as shown in the final output in Fig. 5.3, a second stage DPD is applied on the UL band to suppress it more down and get better ACLR. With 2nd stage DPD, more 10 dB down suppression approximately is achieved in comparison with 1st stage DPD on the UL band, where with this improvement the mission for RF canceller will be easier to reduce the power of the UL band. Fig. 5.4 shows the output of 32 SBFD signals summed together and then an antenna isolation of -80dB is applied, it can be observed from Fig. 5.4 that the nonlinear behavior of the PA is eliminated or in other words, the in band and out of band distortions has been eliminated in all 32 SBFD signal branches. So, the output signal with desired feature is achieved.

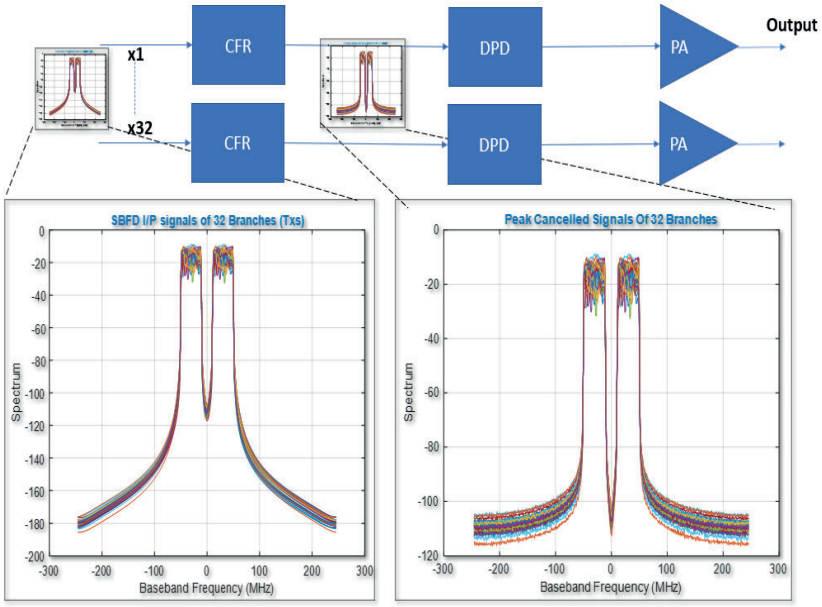

Fig. 5.2. PC-CFR output for 32 branches SBFD input signals (Y-axis: Spectrum power level in dB, X-axis: Baseband frequency in MHz)

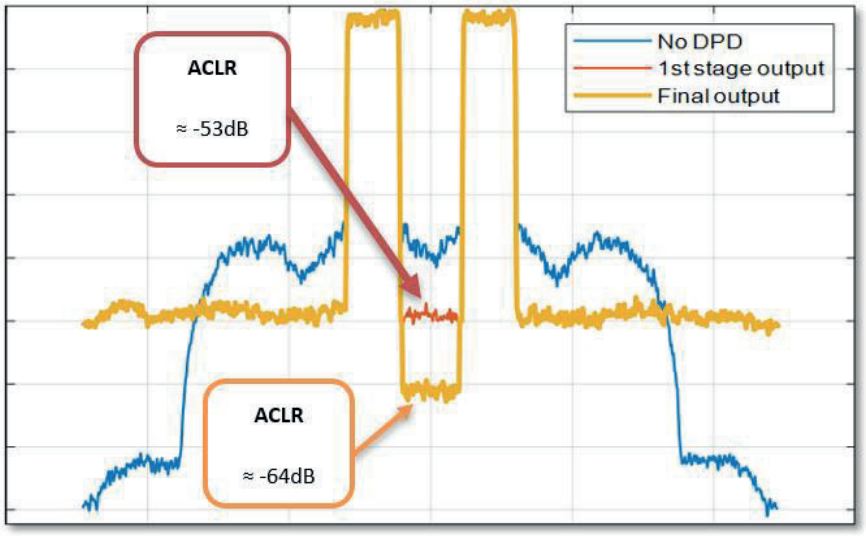

Fig. 5.3. 1st stage DPD and 2nd stage DPD outputs (Y-axis: Spectrum power level in dB, X-axis: Baseband frequency in MHz)

At this moment, transmitted SBFD signal (which constitutes the summation of 32 branches SBFD signals with isolation) will be received from receiver side at the same gNodeB (see Fig. 5.1). As shown in Fig. 5.1, the receiver chain consists of RF Canceller, Low Noise Amplifier (LNA) and Analog to Digital Converter (ADC) blocks. As discussed before, at the receiver chain side SIC technique is implemented, and SIC block is responsible for mitigating interference which is added to the received UL band output signal.

Before going with SIC technique implementation, a link budget calculation must be considered. The link budget is calculated for different values of SNR levels and RF canceller to evaluate the performance of the system with SIC technique. Hence, Signal to Interference Noise Ratio (SINR) is calculated for different values of SNR and RF canceller as will be shown later.

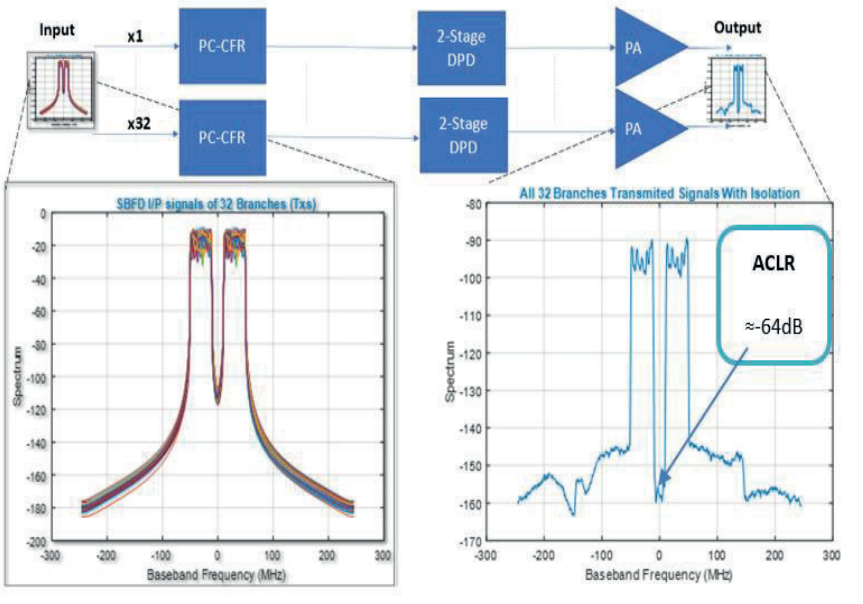

Fig. 5.4. Transmitter side output, Summation of 32 branches SBFD signals with 80dB antenna isolation

Table 5.1 shows the link budget calculations for the received 20 MHz UL band. The noise level is calculated by using thermal noise formula as shown in equation 5.1. Besides, 5 dB Noise Figure (NF) is considered, where NF is the amount of noise power added by the electronic circuitry in the receiver to the thermal noise power from the input of the receiver. Different RF canceller levels (0, 5, 10, 15, and 20 dB) is applied on the received 20 MHz UL band. Different SNR levels (5, 10, 15, and 20 dB) are considered by adjusting the power of the received signal from User Equipment (UE) to evaluate the performance of SIC technique in the designed system.

$$\text{Noise Level} = 10 * \log_{10} (K*T*B) \quad (5.1)$$

Where:

K: Boltzmann constant ($1.38*10^{-23}$ joules/kelvin).

T: Temperature (290 Kelvin).

B: Bandwidth (20MHz).

Table 5.1. Link budget measurement for received 20MHz UL band

UL band (20 MHz)	**Power**
Transmitted power	50 dBm
Isolation (Path Loss)	80 (With random phases) dB
ACLR (1-stage DPD)	53 dB
ACLR (2-stage DPD)	64 dB
RF Canceller	20,15,10,5,0 dB
Noise Figure	5 dB
Noise Level KTB	-101 dBm

From table 5.1, by adding transmitted power to the isolation and then adding ACLR of the 2nd stage DPD, it can be observed that the received UL band signal distortion is -94dBm, which is 7dB higher than the noise level and this will lead to self-interference at the gNodeB. So, more suppression of the UL band is required, and as mentioned before digital RF canceller and SIC technique is applied to suppress more the UL band.

In SIC technique, as shown in Fig. 5.1, the filtered 20 MHz UL band signal, UE interfered signal and Additive White Gaussian Noise (AWGN) signal are added together at the receiver chain side after passing through ADC block. Then, from the result of addition, the filtered UL 20 MHz is subtracted to obtain cancelled self-interference output signal (SIC output) in the UL band, which will lead to allow the SBFD gNodeB to transmit and receive simultaneously. Equation 5.2 describes the calculation to obtain SIC output signal.

$$\text{SIC output} = \text{Average power}\left((\text{UL} + \text{AWGN} + \text{UE}) - (\text{UL}')\right) \quad (5.2)$$

Where:

SIC output: Average power of the self-interference cancelled signal output.

UL: Average power of the UL band.

AWGN: Average power of AWGN signal.

UE: Average power of the interfered signal received from UE.

UL′: Average power of the UL filtered band. Filtered by a digital filter of order 32 as shown in Fig. 5.5.

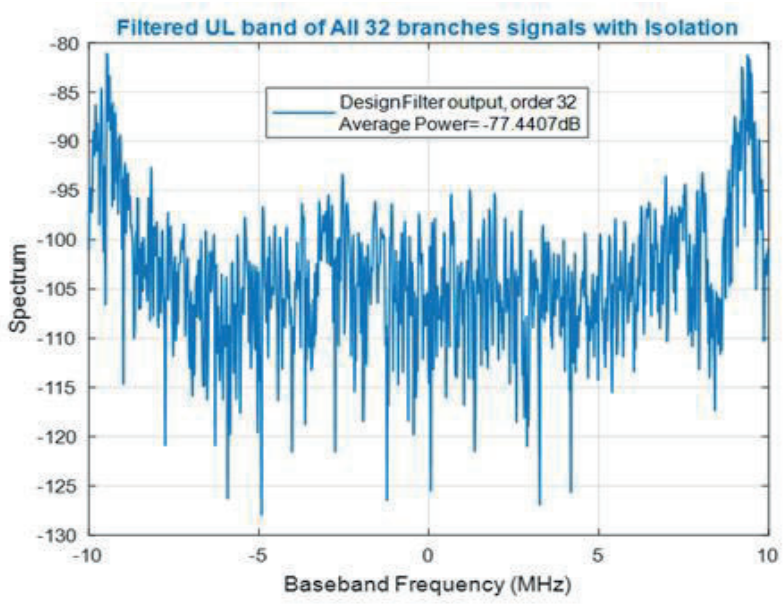

Fig. 5.5. UL band filtered by digital filter of order 32 (Y-axis: Spectrum power level in dB, X-axis: Baseband frequency in MHz).

For more clarification, the signals that we used in our implementation of SIC are shown in the next four figures. Fig. 5.6 shows the AWGN signal at the receiver with average power level of -101dBm. Fig. 5.7 shows the interfered received signal from UE after passing through ADC, with different average power levels adjusted for different required SNR levels. Fig. 5.8 shows the transmitted UL band after passing through ADC, with different power levels referred to different RF cancellation power levels.

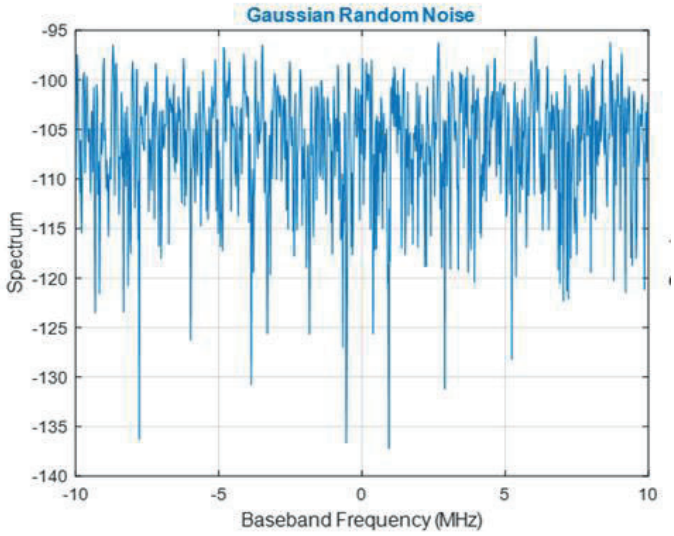

Fig. 5.6. Gaussian noise signal represents the sensitivity (thermal noise) level of the receiver (Y-axis: Spectrum power level in dB, X-axis: Baseband frequency in MHz)

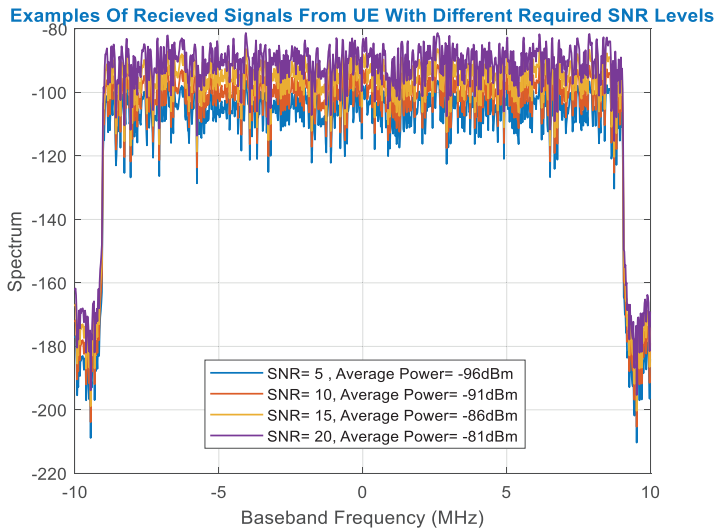

Fig. 5.7. Interfered signal received from UE with different required SNR levels (Y-axis: Spectrum power level in dB, X-axis: Baseband frequency in MHz)

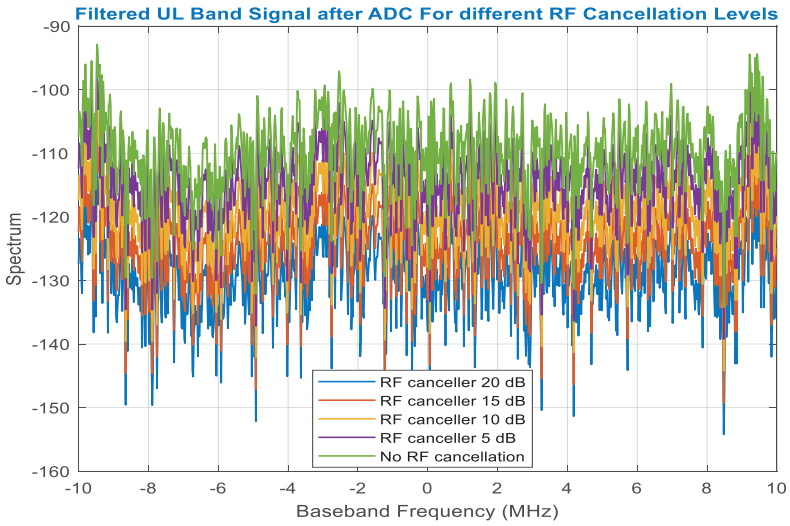

Fig. 5.8. Filtered UL band signals with different RF cancellations levels (Y axis: Spectrum power level in dB, X-axis: Baseband frequency in MHz)

For more clarification of Fig. 5.8, Table 5.2 shows the average power levels for UL band signals with corresponding RF cancellations.

Table 5.2. Average power levels for UL band signals with different RF cancellations levels

RF Cancellation level (dB)	**UL Band Average Power (dBm)**
No RF Cancellation	-77.4
5	-82.4
10	-87.4
15	-92.4
20	-97.4

Finally, Fig. 5.9 shows the SIC output signals with different required SNR levels. Besides, from the average power levels, we can observe an accepted suppression of the UL band signal, and a mitigated self-interference

at gNodeB. In that case SBFD gNodeBs can transmit and receive simultaneously.

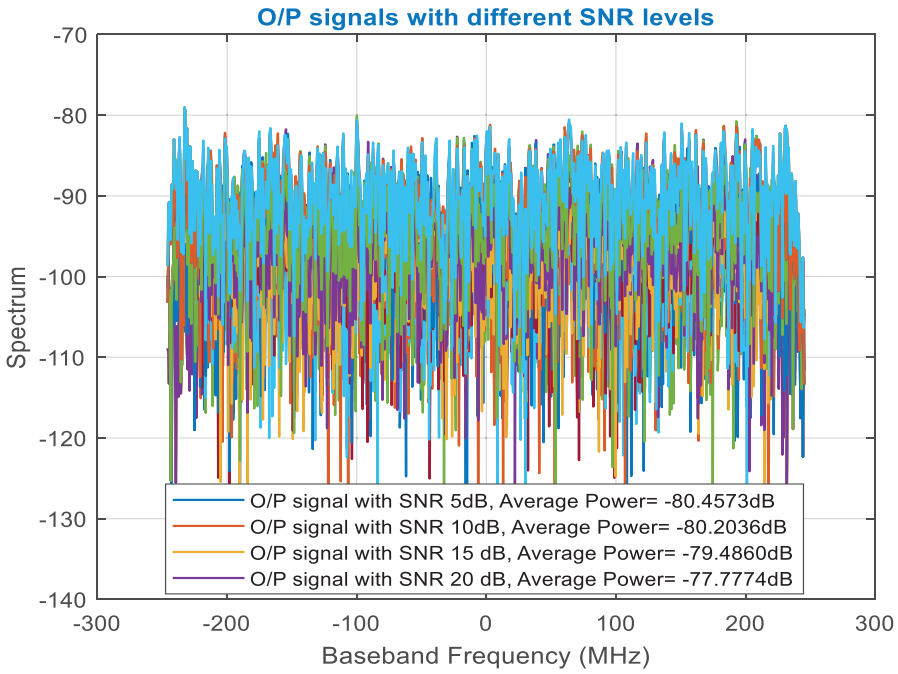

Fig. 5.9. SIC technique output with different required SNR levels and corresponding average power levels (Y-axis: Spectrum power level in dB, X-axis: Baseband frequency in MHz)

In the end, system performance is evaluated by calculating SINRs for different SNR levels, and for different RF cancellation levels on the UL band signal as shown in equation 5.3.

$$\text{SINR} = \text{Average power}\left(\frac{\text{interfered signal (UE signal)}}{\text{SIC output} - \text{interfered signal (UE signal)}}\right) \quad (5.3)$$

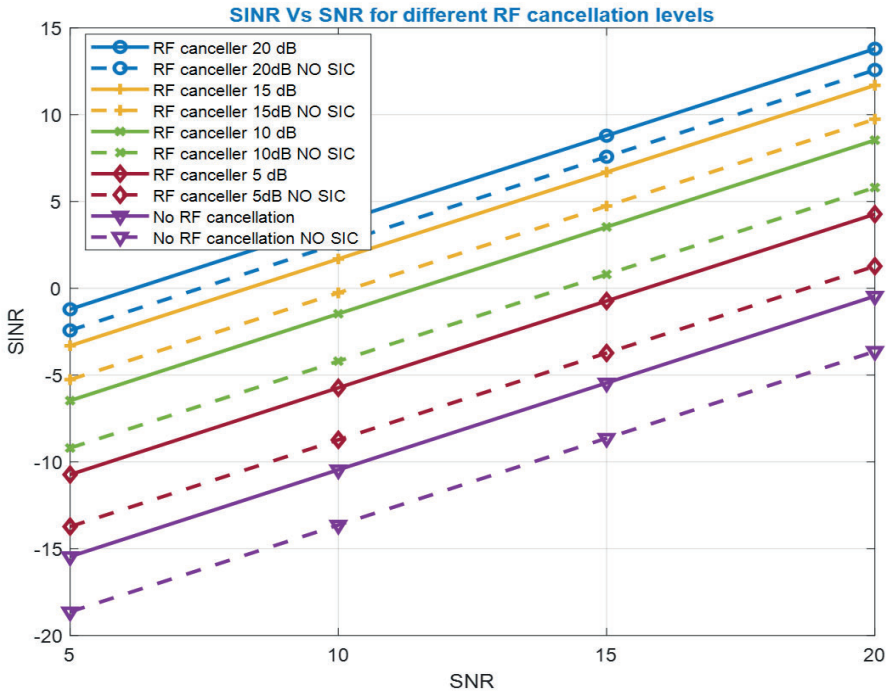

Fig. 5.10. SINR versus SNR for different SNR and RF cancellation levels

Fig. 5.10 shows that SINR is linearly proportional to SNR, for example, Signal with SNR of 20 dB delivers higher SINR than signal with 15 dB. Besides, higher SINR levels are achieved for different SNR levels with applying RF cancellation and SIC technique, which reflects a higher system performance, where UL band is suppressed more, and self-interference is better eliminated. It can be observed from the Fig. 5.10, the continuous blue line shows the highest system performance, where highest SINR levels are achieved for different SNR levels with applying highest RF cancellation level (20 dB) and SIC technique. On other hand, the dashed violet line shows the lowest system performance, where lowest SINR levels are obtained for different SNR levels, since both RF cancellation and SIC technique were not applied to the signal.

6. Conclusion & Future Work

6.1. Conclusion

The modern technology of SBFD for FR1 where very stringent in-band distortion is mitigated to protect UL reception and only conventional DPD algorithms fail to fulfill both the ACLR and power consumption requirement. The algorithms for CFR/DPD for multicarrier power amplifiers are implemented to cancel out-of-band distortions, and in-band distortions by suppressing the UL band spectrum in terms of ACLR and EVM.

The design algorithm for CFR block which is named as the PC-CFR is developed, implemented, and compared with the legacy technique TC and the result shows that PC outperforms the TC due to the specific requirements of our SBFD scenario.

A new technique of DPD which is named as “2-stage frequency selective DPD” is implemented to evaluate the system performance which resulted in better suppression of UL as compared to single DPD block.

SIC technique is developed and evaluated. Different values of SINR are calculated against different SNR and RF cancellation levels. In the end, we observed that the developed SIC system outperforms with SIC and RF cancellation techniques as shown in Fig. 5.10.

6.2. Future Work

With the deployment of the SBFD, the foundation of expected future is already paved. After SBFD success, the new idea is the Single Frequency Full Duplex (SFFD) for FR2. SFFD is a duplex scheme where a simultaneous transmission and reception of DL and UL, respectively, can be obtained on the same frequency resources [1]. The future goals are to identify and evaluate potential enhancements to support duplex evolution of 5G NR specially for TDD.

This thesis is the study and evaluation of the SBFD for non-overlapping sub bands. Future study of partial overlapping and full overlapping sub bands in a real frequency selective channel can be conducted.

In addition, Study inter-gNodeB, inter-device CLI management and impact on RF requirements considering adjacent-channel coexistence with legacy operation. CLI can be present between gNodeBs and between UEs [13].

There are several challenges required to enable the new duplex technology in upcoming NR releases [1]. The mitigation of multiple sources of interference may require some advance techniques in addition to existing ones.

More scenarios and configurations need to be studied and researched with CLI management through spatial domain.

References

[1] QUALCOMM, “On new radio full duplex, perspectives for release 18,” Ericsson internal paper.

[2] Erik Dahlman, Johan Sköld and Stefan Parkvall, “5G NR The Next Generation Wireless Access Technology,”, ISBN 978-0-12-822320-8.

[3] Per Landin, “Digital Baseband Modeling and Correction of Radio Frequency Power Amplifiers”, Doctoral thesis, KTH university, Sweden and VUB university Belgium, June 2012.

[4] Pooria Varaham, https://www.5gtechnologyworld.com/how-dpd-improves-power-amplifier-efficiency/, Feb 2022.

[5] Jessica Chani-Cahuana, Per Niklas Landin, Christian Fager, Thomas Ericsson “Iterative Learning Control For RF Power Amplifiers Linearization”, Communication Systems and Information Theory Group Department of Signals and Systems, Chalmers University of Technology, Gothenburg, Sweden, 2016.

[6] Di Wang, Sumeeth Diddigi “Low Power Pre-Distorter Design For 5G Radio Using Machine Learning”, Master’s Thesis Department of Electrical and Information Technology Lund University, Sept 2020.

[7] Matteo Bernini, “An efficient Hardware Implementation Of The Peak Cancellation Crest Factor Reduction Algorithm”, Master’s Thesis, Department of Information and Communication, KTH Sweden,2016.

[8] Bharadia, Dinesh; McMilin, Emily; Katti, Sachin (2013). "Full duplex radios" (PDF). ACM SIGCOMM Computer Communication Review. **43** (4. 375–386. doi:10.1145/2534169.2486033. Retrieved 2018-04-23.

[9] Choi, Jung Il; Jain, Mayank; Srinivasan, Kannan; Levis, Philip; Katti, Sachin (2010). Achieving single channel, full duplex wireless communication (PDF). MobiCom, 2010. Chicago, IL November 20–24, 2010.

[10] Korpi, D.; AghababaeeTafreshi, M.; Piilila, M.; Anttila, L.; Valkama, M. (2016). Advanced architectures for self-interference cancellation in full-duplex radios: algorithms and measurements (PDF). 50th Asilomar Conference on Signals, Systems, and Computers, 2016. Pacific Grove, CA November 6–9, 2016.

[11] Self-interference cancellation, Self-interference cancellation - Wikipedia.

[12] Ali A. Zaidi, Robert Baldemair, Mattias Andersson, Sebastian Faxér, Vicent Molés-Cases, Zhao Wang, "Designing for the future: the 5G NR physical layer", Ericsson, July 2017.

[13] Qualcomm, "Setting off the 5G Advanced evolution", January 2022, San Diego,CA, www.qualcomm.com.

[14] The electronics designs 70 years, https://www.electronicdesign.com/technologies/communications/article/21801257/electronic-design-whats-the-difference-between-fdd-and-tdd.

[15] [15] Yonis, Aws & Abdullah, Mohammad Faiz Liew & Ghanim, Mayada. (2012). LTE-FDD and LTE-TDD for cellular communications. Progress in Electromagnetics Research Symposium.

[16]

[17]

Printed by Tryckeriet i E-huset, Lund 2023

LUND
UNIVERSITY

Series of Master´s theses
Department of Electrical and Information Technology
LU/LTH-EIT 2023-913
http://www.eit.lth.se